NREL
NATIONAL RENEWABLE ENERGY LABORATORY

Evaluation of Clear Sky Models for Satellite-Based Irradiance Estimates

Manajit Sengupta and Peter Gotseff
National Renewable Energy Laboratory

NREL is a national laboratory of the U.S. Department of Energy
Office of Energy Efficiency & Renewable Energy
Operated by the Alliance for Sustainable Energy, LLC

This report is available at no cost from the National Renewable Energy Laboratory (NREL) at www.nrel.gov/publications.

Technical Report
NREL/TP-5D00-60735
December 2013

Contract No. DE-AC36-08GO28308

NREL
NATIONAL RENEWABLE ENERGY LABORATORY

Evaluation of Clear Sky Models for Satellite-Based Irradiance Estimates

Manajit Sengupta and Peter Gotseff
National Renewable Energy Laboratory

Prepared under Task No. SS13.8041

NREL is a national laboratory of the U.S. Department of Energy
Office of Energy Efficiency & Renewable Energy
Operated by the Alliance for Sustainable Energy, LLC

This report is available at no cost from the National Renewable Energy Laboratory (NREL) at www.nrel.gov/publications.

National Renewable Energy Laboratory
15013 Denver West Parkway
Golden, CO 80401
303-275-3000 • www.nrel.gov

Technical Report
NREL/TP-5D00-60735
December 2013

Contract No. DE-AC36-08GO28308

NOTICE

This report was prepared as an account of work sponsored by an agency of the United States government. Neither the United States government nor any agency thereof, nor any of their employees, makes any warranty, express or implied, or assumes any legal liability or responsibility for the accuracy, completeness, or usefulness of any information, apparatus, product, or process disclosed, or represents that its use would not infringe privately owned rights. Reference herein to any specific commercial product, process, or service by trade name, trademark, manufacturer, or otherwise does not necessarily constitute or imply its endorsement, recommendation, or favoring by the United States government or any agency thereof. The views and opinions of authors expressed herein do not necessarily state or reflect those of the United States government or any agency thereof.

This report is available at no cost from the National Renewable Energy Laboratory (NREL) at www.nrel.gov/publications.

Available electronically at http://www.osti.gov/bridge

Available for a processing fee to U.S. Department of Energy and its contractors, in paper, from:

U.S. Department of Energy
Office of Scientific and Technical Information
P.O. Box 62
Oak Ridge, TN 37831-0062
phone: 865.576.8401
fax: 865.576.5728
email: mailto:reports@adonis.osti.gov

Available for sale to the public, in paper, from:

U.S. Department of Commerce
National Technical Information Service
5285 Port Royal Road
Springfield, VA 22161
phone: 800.553.6847
fax: 703.605.6900
email: orders@ntis.fedworld.gov
online ordering: http://www.ntis.gov/help/ordermethods.aspx

Cover Photos: (left to right) photo by Pat Corkery, NREL 16416, photo from SunEdison, NREL 17423, photo by Pat Corkery, NREL 16560, photo by Dennis Schroeder, NREL 17613, photo by Dean Armstrong, NREL 17436, photo by Pat Corkery, NREL 17721.

Printed on paper containing at least 50% wastepaper, including 10% post consumer waste.

Table of Contents

Abstract **5**
1 Background **5**
2 Clear Sky Model Conversion to MATLAB **6**
2.1 Model Conversion 6
2.2 Model Validation 7
3 Model Sensitivity **12**
4 Clear Sky Model Performance **13**
4.1 Model Inputs 13
4.1.1 Surface Measurement Inputs 13
4.1.2 Satellite-Based Model Inputs 15
4.2 Model Results 15
4.2.1 Clear Sky Results 15
4.2.2 Model Run Times 19
5 Model Selection and Conclusions **20**
References **21**
Appendix A **22**
Optical Depth Effect on Irradiance 22
Determination of Angstrom Turbidity Coefficients for Model Validation 23
Appendix B **26**
Appendix C **27**
Model Improvement Due to Use of Daily AOD and Half-Hour Water Column 27
Appendix D **29**
GHI Clear Sky Model Comparisons for All Sites 29

This report is available at no cost from the National Renewable Energy Laboratory (NREL) at www.nrel.gov/publications.

Abstract

This report describes an intercomparison of three popular broadband clear sky solar irradiance model results with measured data, as well as satellite-based model clear sky results compared to measured clear sky data. The authors conclude that one of the popular clear sky models (the Bird clear sky model developed by Richard Bird and Roland Hulstrom) could serve as a more accurate replacement for current satellite-model clear sky estimations. Additionally, the analysis of the model results with respect to model input parameters indicates that rather than climatological, annual, or monthly mean input data, higher-time-resolution input parameters improve the general clear sky model performance.

1 Background

The existing Satellite Algorithm for the Shortwave Radiation Budget (SASRAB) Geostationary Operational Environmental Satellite (GOES)-based irradiance model for solar resource assessment has been shown to underestimate direct normal irradiance (DNI) and global horizontal irradiance (GHI) under clear sky conditions, and especially during low solar zenith angle conditions. The reason for this underestimate is that the SASRAB algorithm requires a background reflectance field to calculate solar insolation for the current image. This is generated by recording the second-darkest value for each image pixel over the previous 28 days. This is a visible channel measurement that has been shown to be adversely affected by the earth's surface reflectivity. Thus, desert environments, snow, or any high-albedo conditions that existed at the time of the background calibration force the model to assume it was actually due to high atmospheric aerosols. The result is that the SASRAB clear sky shortwave radiation results will often be underestimated compared to the actual surface radiation. At the time of this algorithm's development in the early 1980s, aerosol content over land via satellite imagery did not exist. However, with satellite aerosol data now available, the opportunity exists to correct the current and historical SASRAB data.

The work presented here is the first part of an effort to implement an improved clear sky algorithm for calculating shortwave GHI and DNI during times when retrievals from the satellite imagery indicate clear skies. In this work, the GHI and DNI from three industry-accepted clear sky models are computed and quantitatively compared to the current implementation of the satellite-based predicted radiation. Satellite image surface locations have been chosen to coincide with the National Oceanic and Atmospheric Administration (NOAA) Surface Radiation Budget Network (SURFRAD) ground stations to allow validation with measured radiation at the earth's surface.

The three models chosen for comparison are the Simplified Solis Broadband (SolisBB) clear sky model developed by Pierre Ineichen [1], the Bird clear sky model developed by Richard Bird and Roland Hulstrom [2], and the REST2 model developed by Chris Gueymard [3]. Each model required conversion from its native format to the Mathworks/MATLAB scripting language and was validated against the results from existing Microsoft Excel spreadsheets or FORTRAN code before their final intercomparison for this work.

This report is available at no cost from the National Renewable Energy Laboratory (NREL) at www.nrel.gov/publications.

2 Clear Sky Model Conversion to MATLAB

2.1 Model Conversion

The clear sky models were converted to a vectorized MATLAB form using the sources listed in Table 1 as a starting point. These sources include the original model in Excel or FORTRAN format and the respective original literature describing the development of each model.

Table 1. Clear Sky Model Validation Sources

Clear Sky Model	Author(s)	Validation Source	MATLAB File Name	Reference
Bird	R. Bird, R. Hulstrom	BIRD_10_04_2011.xls*	pvl_clearsky_bird.m	[1]
SolisBB	P. Ineichen	solis-2008-tool.xls*	pvl_clearsky_solisbb.m	[2]
REST2	C. Gueymard	REST2_v8.5_PC.f*	pvl_clearsky_rest2.m	[3]
*Obtained via private communication				

In order to build a common input data structure for each model, the input format was designed around Sandia National Laboratories' PV_LIB Toolbox for MATLAB [4]. PV_LIB is a collection of subroutines used for photovoltaic (PV) performance modeling that also includes the solar position and translation algorithms that are used throughout this work. All converted models use the PV_LIB Time (year, month, day, hour, minute, second) and Location (latitude, longitude, elevation) structure. However, each model uses a slightly different subset of input atmospheric parameters. In order to make the models consistent as callable subroutines, all the atmospheric parameters are passed in as a named structure. Each model then uses its respective parameters. Each parameter in this structure is a vector of the same length as the Time structure. Key parameters and important assumptions used by each of three clear sky models are summarized in Table 2. Some important notes regarding these inputs include: a) The solar constant used by each model is listed because accepted values have changed over the years and are reflected in each model's development; b) The annual variation in extraterrestrial DNI is calculated using the PV_LIB function *pvl_extraradiation* for the Bird and REST2 models, but SolisBB uses an internal calculation. The result is less than +-0.8 W/m^2 extraterrestrial DNI difference over the course of a year between the two methods; c) The solar zenith angle calculation used in the model may be either geometric or apparent. The geometric sun position angle is based purely on earth-sun geometry, whereas the apparent sun position angle accounts for atmospheric diffraction and can introduce corrections from 0.3° to 1.5° at very high geometric zenith angles from 85° to 92°. The apparent and geometric sun positions are discussed in more detail in Section 2.2.

This report is available at no cost from the National Renewable Energy Laboratory (NREL) at www.nrel.gov/publications.

Table 2. Key Model Input Requirements

Model Property	Bird	SolisBB	REST2
Solar Constant, En [W/m^2]	1367 (corresponds to mult = 0.9751; see [1])	1367	1361.2
Extraterrestrial DNI Annual Variation	*pvl_extraradiation*	Internal	Modified *pvl_extraradiation* to match En = 1361.2
Zenith Angle Calculation	Apparent	Geometric	Apparent
Surface Pressure	Required by *pvl_ephemeris*, *pvl_absoluteairmass*	Required by *pvl_ephemeris*	Required by *pvl_ephemeris*
Surface Temperature	Required by *pvl_ephemeris*	Required by *pvl_ephemeris*	Required by *pvl_ephemeris*
Surface Albedo	Required	Assumed fixed 0.20	Required
Aerosol Optical Depth	380 nm, 500 nm required	700 nm required	Uses α_1, α_2, β below
Ang Turb Coeff (<7 µm), α_1	N/A	N/A	Required (typical 1.3)
Ang Turb Coeff (>7 um), α_2	N/A	N/A	Required (= α_1 if no other info available) (typical 1.3)
β (AOD Intercept at 1 µm)	N/A	N/A	Required
H_2O Vapor [cm]	Required (typical 0.5–5)	Required (typical 0.5–5)	Required (typical 0.5–5)
O_3 [cm]	Required (typical 0.3)	Assumed 0.340	Required (typical 0.3)
NO_2 [cm]			Optional (default 2E-4)
% Forward Scatter Ba	Optional (default 0.84)	Required (default 0.84)	Uses scatter albedo below
Single Scatter Albedo (<7 µm), ω_1	N/A	N/A	Required (typical 0.92)
Single Scatter Albedo (>7 µm), ω_2	N/A	N/A	Required (typical 0.84)

2.2 Model Validation

Once all the models were converted to MATLAB, they were cross checked against the validation sources listed in Table 1. As a final check, each validation source (e.g., Excel worksheet or FORTRAN program) was modified to represent a full year of hourly daytime (zenith angle < 85°) clear sky results. The same input datasets, including time, location (Table Mountain, Colorado, was arbitrarily chosen), zenith angle, elevation, air mass, extraterrestrial radiation, and the atmospheric parameters listed in Table 3, were input to each of the three models. The exception was the REST2 model written in FORTRAN: here, the solar position was calculated internally by the SunPSA subroutine [5], which closely matches the PV_LIB *pvl_ephemeris* results.

The literature for all the clear sky models does not specify whether they are designed for geometric solar position or refracted solar position. Review of Gueymard's REST2 FORTRAN code shows it uses a refracted sun angle obtained from the independently developed SunPSA

This report is available at no cost from the National Renewable Energy Laboratory (NREL) at www.nrel.gov/publications.

subroutine [5]. Ineichen reports that the SolisBB model is designed around geometric sun elevation. The Bird model uses geometric solar position, but it should be noted that calculation of air mass uses the Kasten air mass correction formula, which produces refraction-corrected (apparent) air mass. In the end, all three models correct for the sun's refraction through the atmosphere at some point, which becomes more important at zenith angles greater than 85°. Properly calculating air mass determines the thickness of the atmosphere for a given solar position. All the atmospheric properties (i.e., aerosol, H_2O, O_3, etc.) are then scaled by the air mass and used to determine the transmittance through each component.

Table 3 shows the input parameters used for the model conversion validations. The aerosol optical depth (AOD) values as well as the Angstrom turbidity coefficients are all internally consistent with the annual climatological values at the SURFRAD Table Mountain site. AOD calculations and their relationship to the Angstrom coefficients, α and β, are discussed in Section 4.1.1.

Table 3. Model Input Parameters for Conversion Validation

Latitude/Longitude/Elevation	40.125°/-105.237°/1689 m
Surface Pressure/Temperature	831.31 mPa/15.67°C
Surface Albedo	0.2
H_2O Vapor	0.5 atm-cm
O_3	0.3 atm-cm
NO_2	0.0002 atm-cm
% Forward Scatter Ba	0.84
AOD380/AOD500/AOD700	0.1306/0.0985/0.0706
α_1, α_2, β	0.9174/0.9174/0.0502
ω_1, ω_2	0.92/0.84

The model differences in W/m^2 between the new MATLAB models and the original source models are shown in Figure 1 through Figure 6. All show relatively good agreement. The SolisBB conversion shows nearly perfect agreement with no observable bias beyond what are likely numerical precision differences between MATLAB and Excel. The Bird conversion shows a strong zenith response for clear sky DNI with differences up to +0.045 W/m^2 and to a lesser extent for GHI differences up to +0.021 W/m^2. Finally, the REST2 model shows the largest differences, +2 W/m^2 for DNI and +0.7 W/m^2 for GHI. This has been tracked to the differences in the apparent sun position calculations performed in the solar position algorithms used by REST2 (SunPSA) and PV_LIB *pvl_ephermeris*, which is an implementation of an undocumented solar position algorithm. The differences between the model validation source and MATLAB version were deemed acceptable for all three models.

This report is available at no cost from the National Renewable Energy Laboratory (NREL) at www.nrel.gov/publications.

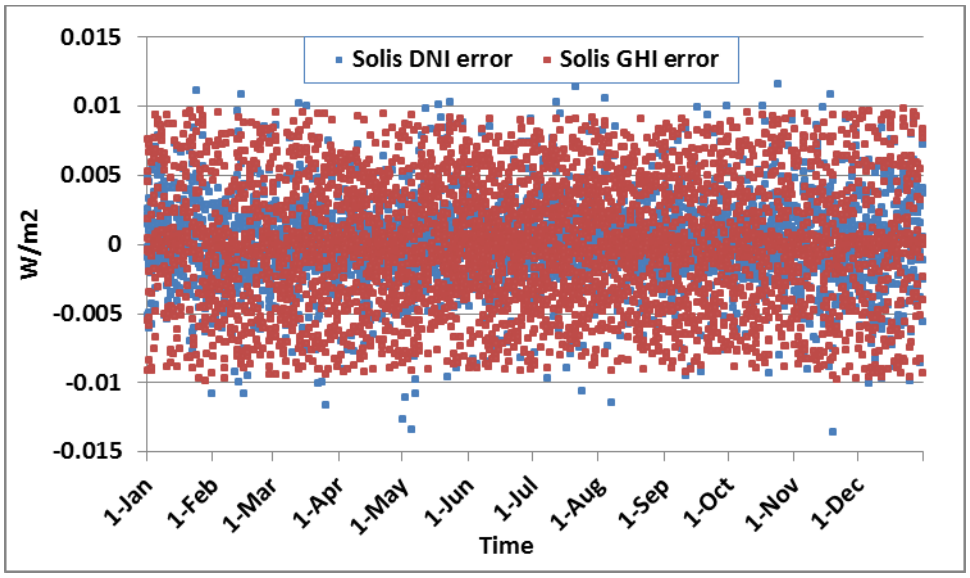

Figure 1. SolisBB chronological model error [W/m^2] between MATLAB and original source.

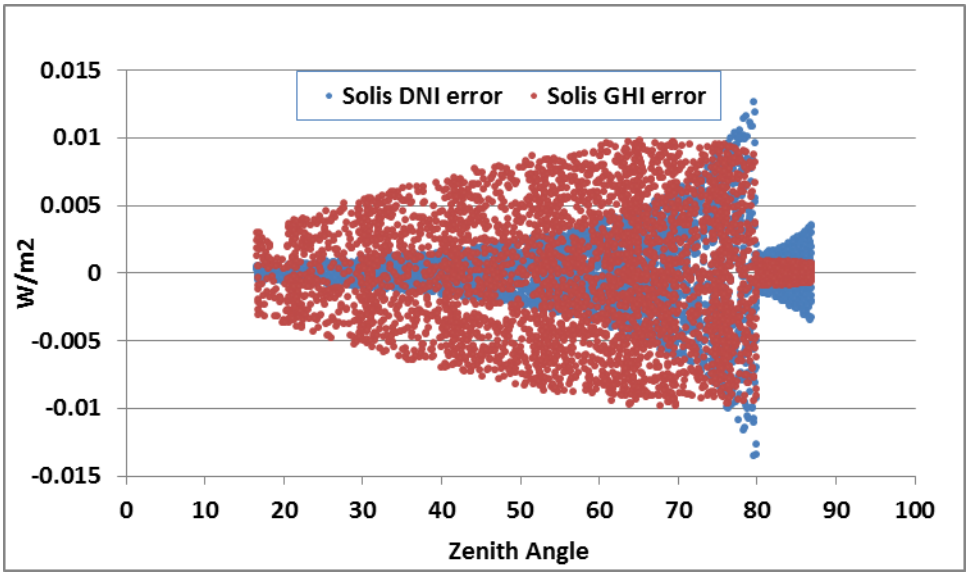

Figure 2. SolisBB model error [W/m^2] between MATLAB and original source vs. zenith angle.

This report is available at no cost from the National Renewable Energy Laboratory (NREL) at www.nrel.gov/publications.

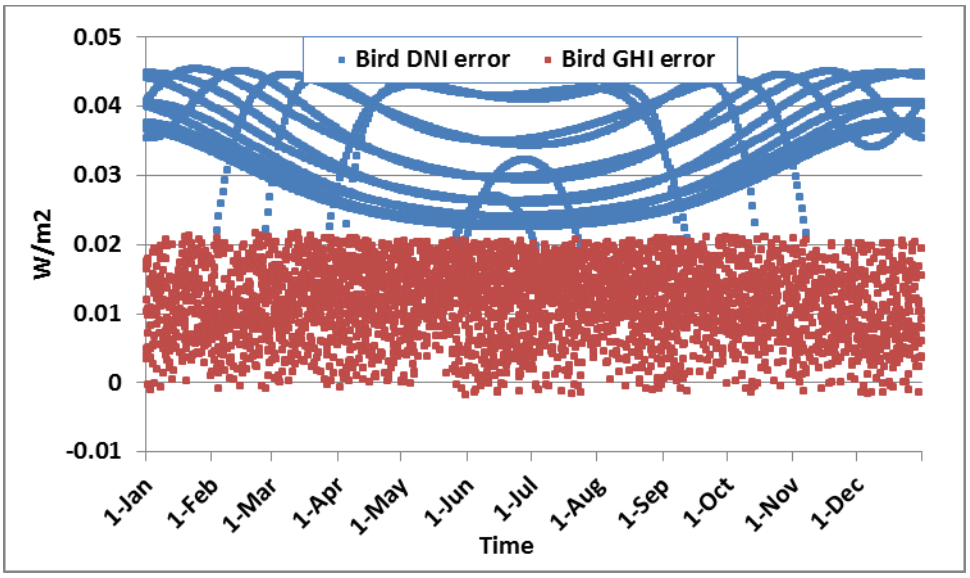

Figure 3. Bird chronological model error [W/m^2] between MATLAB and original source vs. time.

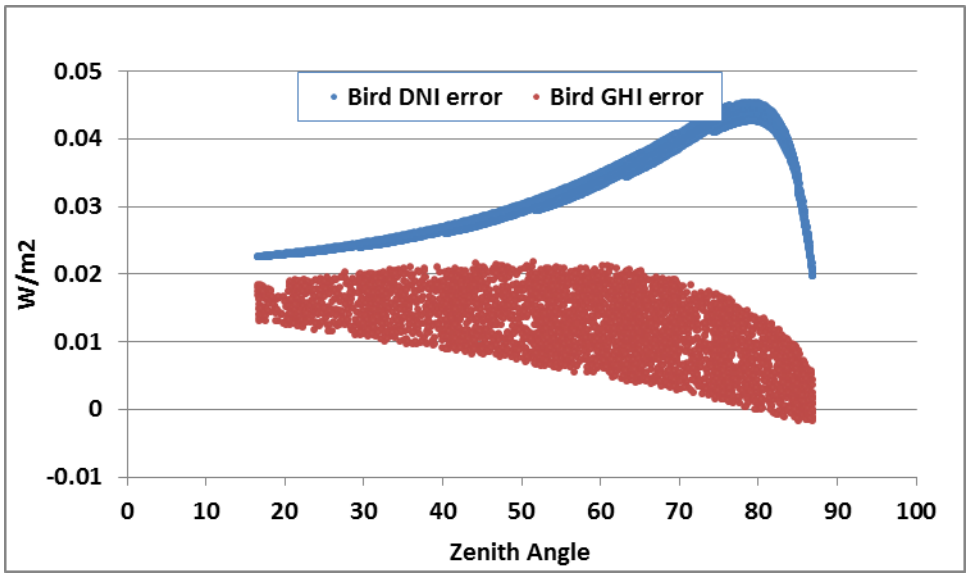

Figure 4. Bird model error [W/m^2] between MATLAB and original source vs. zenith angle.

This report is available at no cost from the National Renewable Energy Laboratory (NREL) at www.nrel.gov/publications.

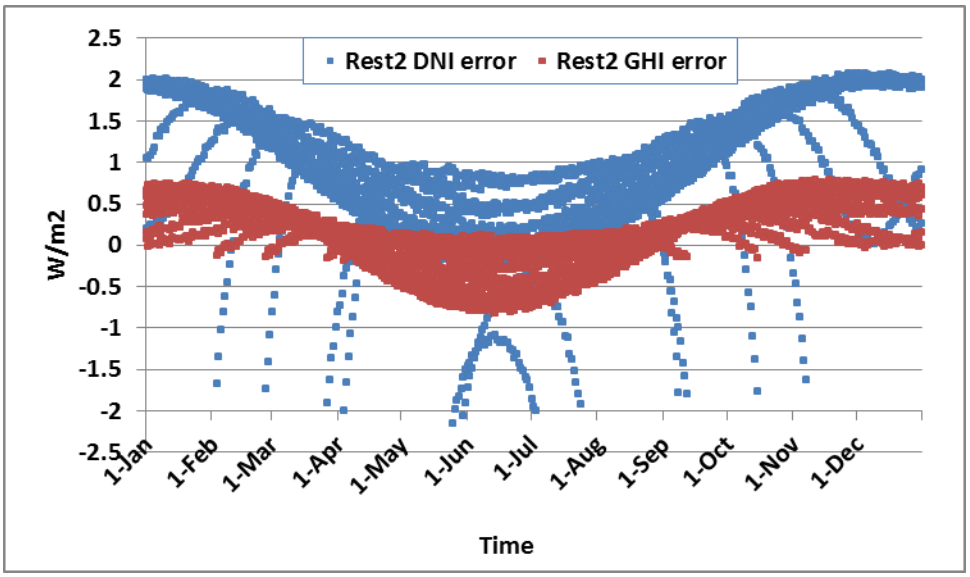

Figure 5. REST2 model error [W/m^2] between MATLAB and original source vs. time.

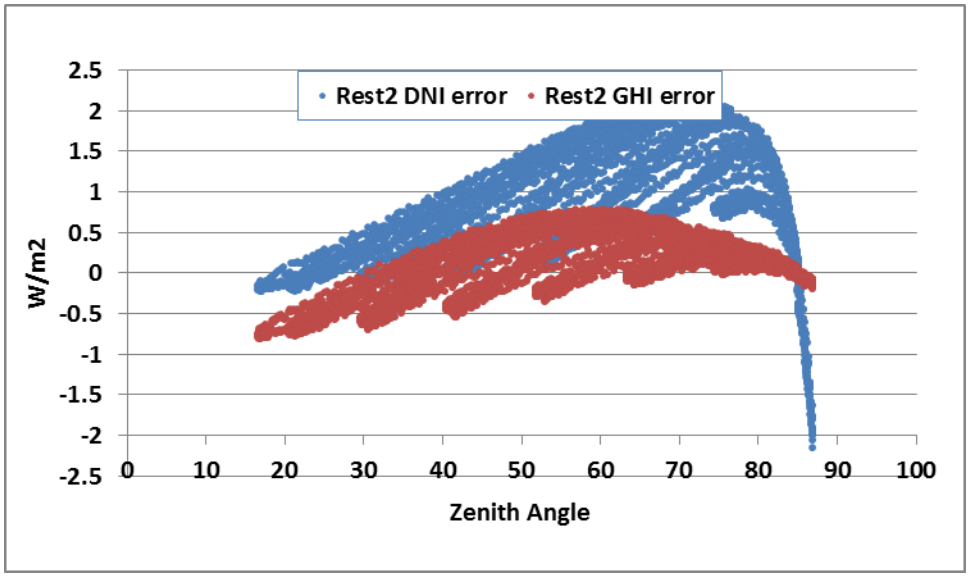

Figure 6. REST2 model error [W/m^2] between MATLAB and original source vs. zenith angle.

In the following sections, the model sensitivities with atmospheric input parameters are presented, and then each model's respective performance is analyzed with respect to surface measurements.

This report is available at no cost from the National Renewable Energy Laboratory (NREL) at www.nrel.gov/publications.

3 Model Sensitivity

This section provides a general idea of how the clear sky models vary with atmospheric conditions. In general, all three models vary in the same manner for a given set of model inputs. For this analysis the Bird model is chosen to show model response, in order of decreasing sensitivity, to: AOD, water column, ozone, forward scattering ratio, and albedo at a fixed air mass of 1.5 (zenith angle = 48.2°) and site location equivalent to Desert Rock, Nevada (latitude 36.63°, longitude -116.02°, elevation 1,007 m).

Figure 7 clearly shows that for the typical ranges encountered for most sites, AOD is the strongest driver of clear sky determination, followed by water column. Thus, to calculate accurate clear skies, the AOD (or alternatively the Angstrom turbidity coefficients) and water column are the two most important parameters to specify correctly. This is especially relevant for the DNI radiation estimate. For example, over the expected range of AOD at 380 nm the modeled GHI can vary up to 80 W/m^2. However, the modeled DNI can vary up to 225 W/m^2, the physical reason being that DNI transmission extinction is strongly driven by aerosol absorption and scattering. Appendix A contains more information on the rate of extinction of radiation for the most relevant atmospheric properties, such as Raleigh scattering, AOD, water vapor, and ozone.

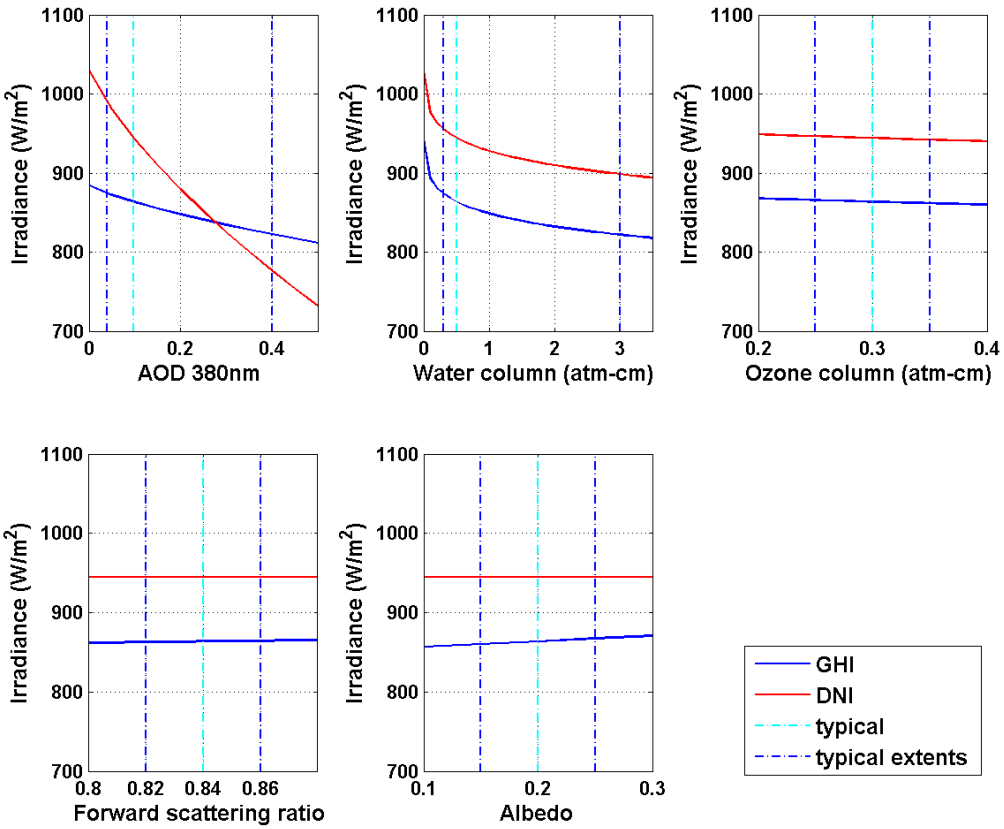

Figure 7. Sensitivity of Bird Model GHI and DNI to atmospheric properties.

This report is available at no cost from the National Renewable Energy Laboratory (NREL) at www.nrel.gov/publications.

4 Clear Sky Model Performance

The relative improvement in performance of the three newly converted clear sky models over the current SASRAB clear sky algorithm is quantified in this section. For this work, seven continental NOAA SURFRAD ground measurement sites were used to quantify the performance of each of the clear sky models over the SASRAB clear sky estimates for the year 2009. These seven sites represent varying mid-latitude continental atmospheric sky conditions from the desert southwest (Desert Rock, Nevada) to the high-humidity south (Goodwin Creek, Mississippi). NOAA also has nine Integrated Surface Irradiance Study (ISIS) measurement stations that are well distributed throughout the United States, but their use here was rejected due to a lack of ground-based AOD measurements required for clear sky model input. The complete list of SURFRAD sites is given in Section 4.1.1. The data flow for this work is detailed in Appendix B.

4.1 Model Inputs

4.1.1 Surface Measurement Inputs

The seven NOAA SURFRAD sites supplying broadband radiation (GHI and DNI) at one-minute intervals are used for quantifying the clear sky model performance. In addition, the co-located surface meteorological measurements (surface pressure, temperature, relative humidity, wind speed, and direction) as well as AOD measurements are used to create more accurate site-specific model inputs to the clear sky models. This allows the models to be evaluated with the best available surface data for determining local atmospheric conditions as model input.

The SURFRAD sites used for analysis are shown in Table 4 along with the latitude and longitude of the center of the assigned 4-km SASRAB grid point and the GOES source for the imagery.

Table 4. SURFRAD Sites Used for Model Performance Analysis

SURFRAD Site (abbreviated name)	SURFRAD Latitude/Longitude	SASRAB Latitude/Longitude	GOES Source
Table Mountain, CO (tbl)	40.125/-105.237	40.109°/-105.257°	West
Desert Rock, NV (dra)	36.62/-116.02	36.643°/-116.030°	West
Goodwin Creek, MS (gwn)	34.25/-89.87	34.267°/-89.870°	East
Penn State, PA (psu)	40.72/-77.93	40.700°/-77.900°	East
Bondville, IL (bnd)	40.05/-88.37	40.051°/-88.327°	East
Fort Peck, MT (fpk)	48.31/-105.1	48.335°/-105.065°	West
Sioux Falls, SD (sxf)	43.73/-96.62	43.732°/-96.600°	East

The SURFRAD GHI and DNI solar irradiance are preprocessed to align properly with the instantaneous GOES images that are taken twice hourly at :00 and :30 past the hour for GOES West and at :15 and :45 past the hour for GOES East. That is, the one-minute SURFRAD irradiance is 30-minute time-averaged on the center of the corresponding GOES image timestamp.

AOD measurements are determined from the co-located Multi-Filter Rotating Shadowband Radiometer (MFRSR) (Harrison, Michalsky, Berndt, 1994). Because each clear sky model requires AOD at different wavelengths, the following approach was used for this analysis. The MFRSR measures AOD wavelengths at: 415 nm, 501 nm, 616 nm, 672 nm, and 868 nm. As stated earlier, the Bird model uses AOD at 380 nm and 500 nm, SolisBB uses AOD at 700 nm, and REST2 uses the Angstrom Law coefficients β, the Angstrom turbidity coefficient, and α, the

This report is available at no cost from the National Renewable Energy Laboratory (NREL) at www.nrel.gov/publications.

Angstrom exponent, to describe atmospheric turbidity. For this analysis the Angstrom coefficients were calculated for the REST2 model, and using those values, the AODs were back calculated for Bird (380 nm, 500 nm) and SolisBB (700 nm) to ensure that all AODs were internally consistent and described the same atmospheric turbidity conditions. A more detailed background on atmospheric turbidity and the Angstrom coefficient calculations is given in Appendix A.

Additionally, co-located temperature and relative humidity are also used to determine atmospheric water column based on the method by Gueymard [6]. This is preprocessed on the same time scale as the irradiance data to coincide with the satellite image.

The variation of surface-measured AOD and half-hour estimated water column over the 2009 evaluation period for each SURFRAD site is shown in Figure 8 with the mean value shown in blue, standard deviation shown as asterisks, and maximum and minimum values shown as red dots. This figure provides a visual clue to how much these two atmospheric parameters can vary over a year for a site.

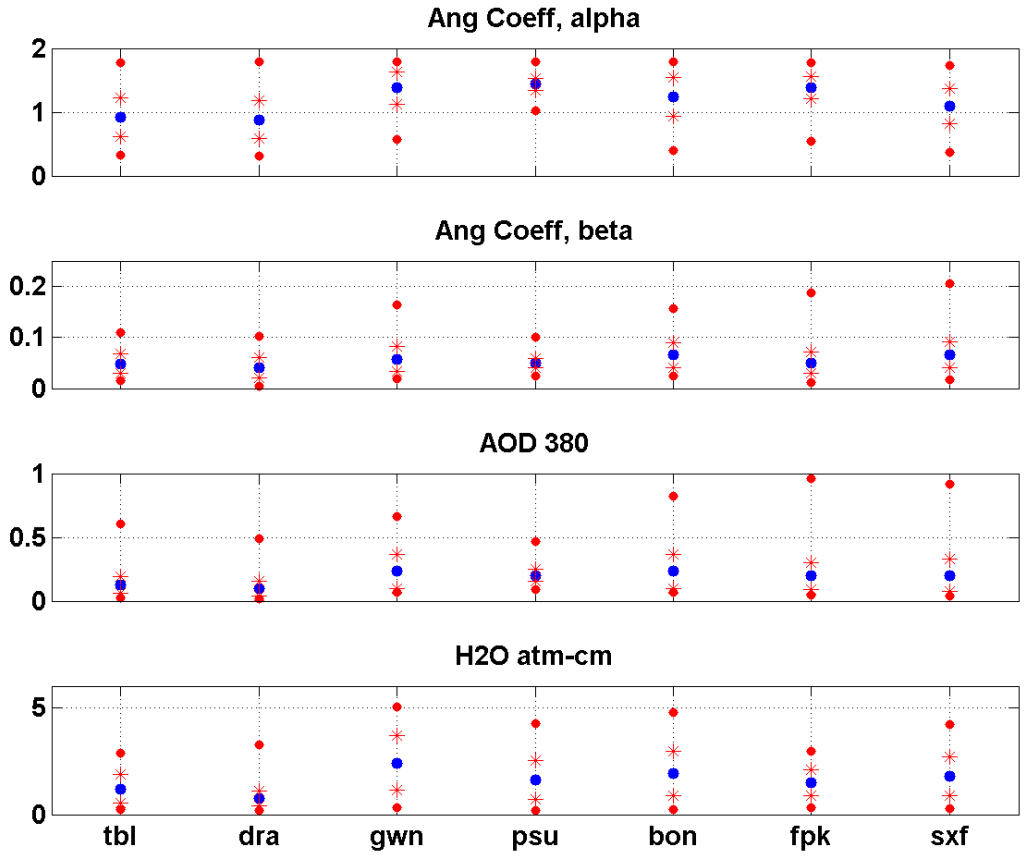

Figure 8. Atmospheric input parameter statistics for AOD and water column.

This report is available at no cost from the National Renewable Energy Laboratory (NREL) at www.nrel.gov/publications.

4.1.2 Satellite-Based Model Inputs

The GOES-based PATMOS-X/SASRAB product makes over 50 measured atmospheric parameters available in self-contained Hierarchical Data Format (HDF) files. However, for this analysis only the calculated *insolation* (GHI), *insolation_diffuse* (DHI), and *cloud_type* are used. Furthermore, this analysis is restricted to clear skies as determined by SASRAB. This is equivalent to those satellite image pixels where *cloud_type* is identified as "0."

The nearest GOES East or GOES West satellite pixel corresponding to a SURFRAD location is used to extract calculated insolation and cloud type for analysis. The SURFRAD site and corresponding SASRAB pixel (identified by latitude and longitude) used in this analysis are shown in Table 4.

The satellite *cloud_type* is the primary filter for identifying clear skies with a secondary requirement that the satellite reported zenith angle be less than 85°. This threshold is intended to eliminate the highest zenith angles (sunrise and sunset). The times of all half-hour SASRAB data that pass these criteria are then intersected with the corresponding half-hour averaged SURFRAD data for subsequent processing of the 2009 analysis year.

4.2 Model Results

4.2.1 Clear Sky Results

This section illustrates the performance differences between the three clear sky models compared to the SURFRAD measurements for clear sky conditions as identified by the SASRAB *cloud_type* index for the 2009 analysis year. Model performance is quantified for each of three models for two input parameter cases: 1) annual climatic values for the AOD and water column model inputs and 2) average daily values for AOD and half-hour water column estimates using the method by Gueymard.

The model sensitivities shown in Section 3 would imply that more accurate AOD and water column would result in the largest clear sky model improvements. The scatter plots in Figure 9 and Figure 10 graphically demonstrate this for the Desert Rock SURFRAD site. This improvement can be seen at all sites and shows the important fact that providing higher-resolution model inputs (here, daily and half-hourly rather than annual climatic values) is critical in accurately estimating clear sky irradiance. For the Desert Rock location, this results in mild improvement in modeled GHI from all three models—improving the average RMSE to 28.0 W/m^2 from 32.5 W/m^2. DNI improvement is striking—improving the model average value to 63.3 W/m^2 from 89.5 W/m^2. Appendix C demonstrates how the clear sky models improve statistically as annual fixed climatic values are replaced with more refined daily AOD or half-hour water column estimates, and Appendix D includes individual scatter plots for all SURFRAD sites. The figures show the modeled vs. measured GHI and DNI for: 1) annual climatic AOD values and water column and 2) daily AOD and half-hour averaged water column—with both parameters derived from the SURFRAD datasets.

This report is available at no cost from the National Renewable Energy Laboratory (NREL) at www.nrel.gov/publications.

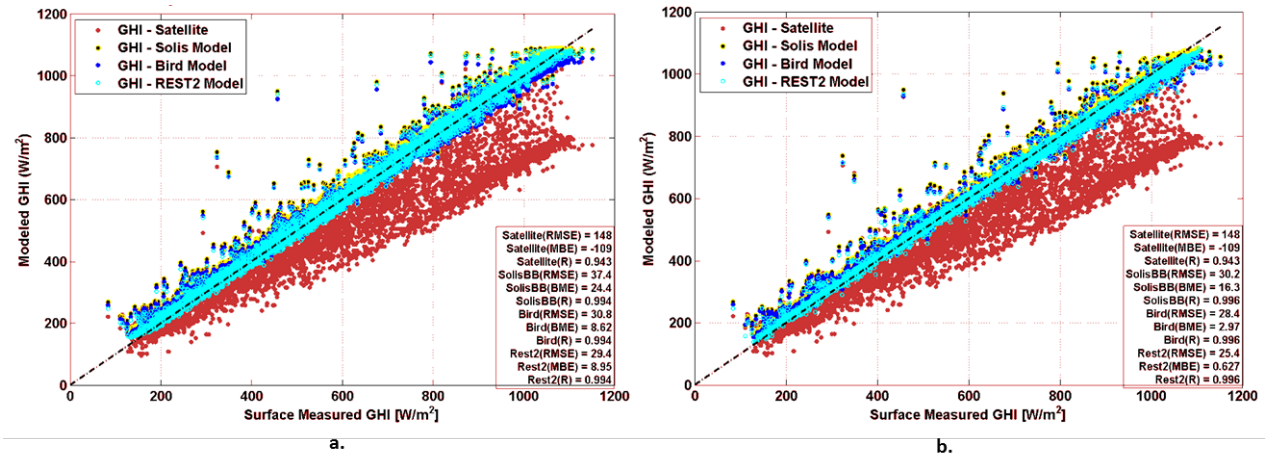

Figure 9. GHI clear sky model comparisons for Desert Rock, Nevada: a) climatic AOD, fixed water column; b) daily AOD, half-hour water column.

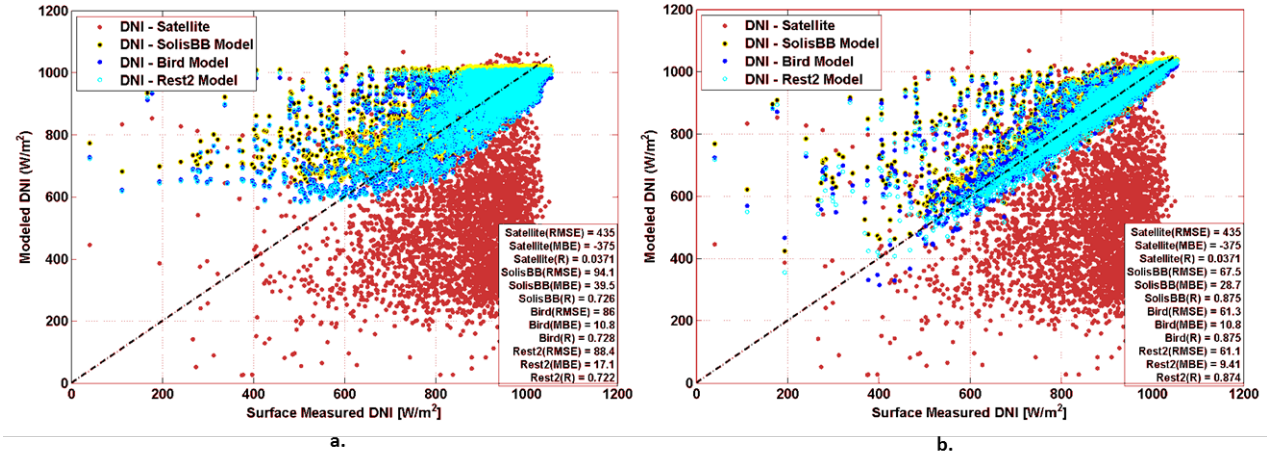

Figure 10. DNI clear sky model comparisons for Desert Rock, Nevada: a) climatic AOD, fixed water column; b) daily AOD, half-hour water column.

The relative performance of each clear sky model is ranked based on summary statistics for the 2009 analysis year using the refined daily model inputs. Figure 11 and Figure 12 bar charts show the statistical performance of each model with respect to the others for each SURFRAD site. Note the different axis limits for both the GHI and DNI statistics, which show that GHI has similar errors irrespective of the model, whereas DNI is more strongly influenced by AOD and water column, and its degree of "correctness" is more strongly dependent on the model being used. This same data is presented in Table 5. Furthermore, Table 6 presents average summary statistics for all SURFRAD sites combined, which are used in final model selection as described in Section 5.

In general, all three clear sky models compare well, with REST2 slightly outperforming Bird and SolisBB for most sites. For most sites, the REST2 root mean square error (RMSE) is typically less than the Bird RMSE by 3 W/m^2 to 10 W/m^2 for GHI, but not significantly different for DNI, with typical site-to-site differences of less than 2 W/m^2.

This report is available at no cost from the National Renewable Energy Laboratory (NREL) at www.nrel.gov/publications.

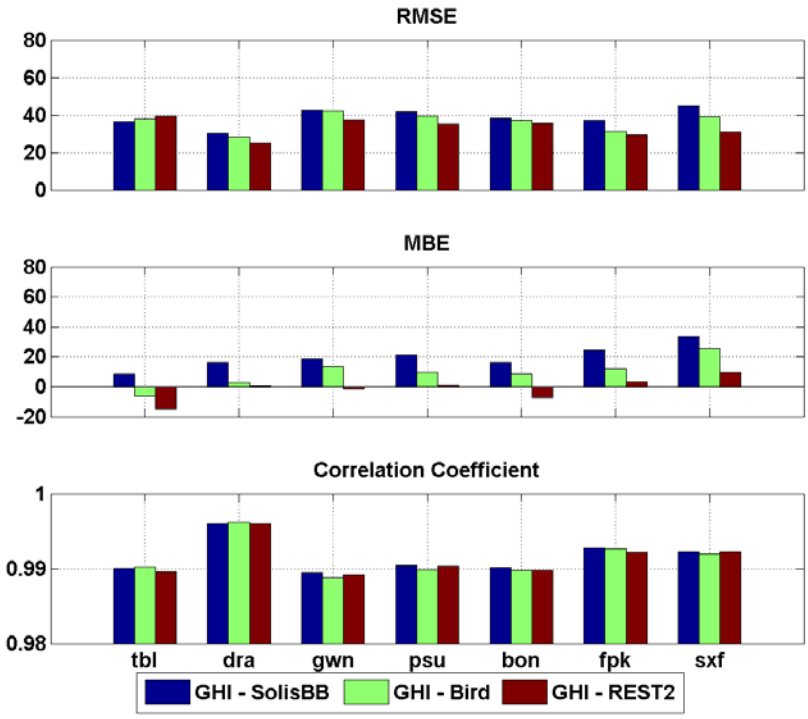

Figure 11**. GHI model error comparisons for daily AOD and half-hour water column.**

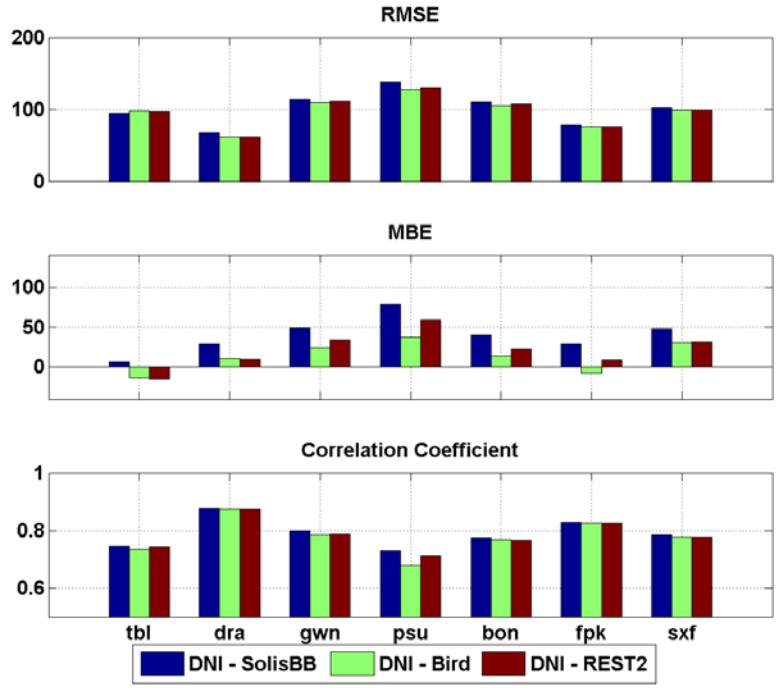

Figure 12. DNI model error comparisons for daily AOD and half-hour water column.

This report is available at no cost from the National Renewable Energy Laboratory (NREL) at www.nrel.gov/publications.

Table 5. Summary Statistics for Individual SURFRAD Sites for Daily AOD, Half-Hour Water Column

SURFRAD Site		GHI [W/m^2]				DNI [W/m^2]			
		SASRAB	SolisBB	Bird	REST2	SASRAB	SolisBB	Bird	REST2
TblMtn, CO	RMSE	102.85	36.35	37.74	39.27	353.90	94.94	97.51	96.36
	MBE	-71.28	8.46	-6.31	-14.76	-266.41	6.05	-13.51	-14.94
	R	0.95	0.99	0.99	0.99	0.08	0.75	0.73	0.74
DesertRock, NV	RMSE	148.08	30.21	28.42	25.36	435.08	67.50	61.34	61.09
	MBE	-109.17	16.30	2.97	0.63	-374.77	28.69	10.84	9.41
	R	0.94	1.00	1.00	1.00	0.04	0.88	0.87	0.87
GoodwinCreek, MS	RMSE	58.88	42.31	42.05	37.69	150.63	113.90	109.20	111.12
	MBE	-7.63	18.88	13.58	-1.55	-11.50	48.44	24.83	34.41
	R	0.97	0.99	0.99	0.99	0.66	0.80	0.78	0.79
PennState, PA	RMSE	86.97	41.69	39.44	35.29	233.88	138.02	127.41	130.33
	MBE	-46.00	21.06	9.78	1.03	-112.35	78.65	37.57	59.49
	R	0.96	0.99	0.99	0.99	0.41	0.73	0.68	0.71
Bondville, IL	RMSE	72.41	38.30	37.19	35.56	199.93	109.98	105.70	107.45
	MBE	-33.42	16.35	8.45	-7.41	-95.67	39.82	14.13	22.92
	R	0.97	0.99	0.99	0.99	0.54	0.77	0.77	0.76
FortPeck, MT	RMSE	54.66	37.20	31.46	29.25	186.46	78.48	75.43	75.12
	MBE	-20.07	24.42	11.86	3.16	-112.45	28.63	-7.80	8.70
	R	0.98	0.99	0.99	0.99	0.59	0.83	0.83	0.83
SiouxFalls, SD	RMSE	60.57	44.68	39.21	30.78	193.14	102.34	98.36	98.29
	MBE	-13.07	33.77	25.37	9.46	-81.13	48.08	30.46	31.68
	R	0.97	0.99	0.99	0.99	0.51	0.79	0.78	0.78

Table 6. Summary Statistics for All SURFRAD Sites Combined

	GHI [W/m^2]			DNI [W/m^2]		
	SolisBB	Bird	REST2	SolisBB	Bird	REST2
RMSE	38.68	36.50	33.31	100.74	96.42	97.11
MBE	19.89	9.39	-1.35	39.76	13.79	21.67
R	0.992	0.991	0.991	0.791	0.777	0.784

The larger DNI RMSE in the statistics and additional scatter in the DNI comparison figures when compared to GHI also reveal an artifact of the analysis method as well as one of the issues with using satellite data. The satellite value is calculated based on an instantaneous pixel image corresponding to a 4-km by 4-km surface, whereas the SURFRAD ground measurements in this study are half-hour averages centered on the time of the satellite image and represent a point measurement. The *cloud_type* index may indicate a clear sky within that pixel at the instant the image was captured, but the measurement average over the half hour may be partly cloudy over that time, lowering the overall average. This affects the GHI, which is a combination of both direct and diffuse irradiance components—but more so the DNI. During partly cloudy conditions, DNI surface measurements can be anywhere between zero and clear sky irradiance within the 30-minute period. As with the GHI, the satellite instantaneous DNI irradiance

This report is available at no cost from the National Renewable Energy Laboratory (NREL) at www.nrel.gov/publications.

estimates are based on some value in that range not necessarily reflecting the half-hour average. Furthermore, there may be no satellite pixel center point directly overhead of the surface measurement point.

4.2.2 Model Run Times

All three clear sky models were evaluated for runtime performance. Results for per-point runtime are listed in Table 7. To clarify, because the models are vectorized in MATLAB, vectors of time, location, and model parameters are passed to each clear sky model. The per-point time is the total function execution time divided by the number of elements in the vectors, excluding the first call to the function, which has been found to have considerable overhead in terms of execution time for all the models. In practice it has been found that the lengths of the input parameter vectors passed to the clear sky models make negligible differences in per-point timing. Thus, this level of performance should be expected for a production version of these models, which will be used to correct the SASRAB clear sky GHI and DNI values.

Table 7. Model Per-Point Timing

Model	Per-Point Time [µsec]
SolisBB	3.95
Bird	4.12
REST2	6.23

This report is available at no cost from the National Renewable Energy Laboratory (NREL) at www.nrel.gov/publications.

5 Model Selection and Conclusions

The summary statistics in Table 6 point to Bird and REST2 as the most promising of the three models for replacing the SASRAB clear sky estimator, with overall RMSE for GHI of 36.50 W/m^2 and 33.31 W/m^2, respectively, and DNI errors of 96.42 W/m^2 and 97.11 W/m^2, respectively. In final production, each SASRAB clear sky satellite pixel value for GHI and DNI will be replaced with one of these models' clear sky values. Thus, runtime will be critical—which leads to the final selection of the Bird model, which runs in two-thirds of the time of REST2. This selection should not preclude the use of REST2 in other applications. This project is solely focused on broadband GHI and DNI values (i.e., wavelengths from .3–3 µm). However, REST2 is spectrally selective and specifically designed to estimate broadband, illuminance, and photosynthetically active radiation (PAR) values that can be used in other disciplines. Furthermore, with some modification by its author, REST2 could provide irradiance values that coincide with particular PV materials' wavelengths (e.g., 0.3–1.1 µm for silicon), which could potentially be useful to more accurately estimate power production from these materials.

Overall conclusions from this work are as follows:

- Any of the three clear sky models used in this analysis is superior to the current SASRAB clear sky model.
- For this analysis, the SASRAB *cloud_type* parameter has been found to be an accurate clear sky identifier.
- High-temporal-resolution model input data parameters such as AOD and water vapor significantly improve clear sky model accuracy.
- The Bird clear sky model combines relatively good performance coupled with computational efficiency.

This report is available at no cost from the National Renewable Energy Laboratory (NREL) at www.nrel.gov/publications.

References

[1] Ineichen, P. "A Broadband Simplified Version of the Solis Clear Sky Model." *Solar Energy* (82:8), 2008; pp. 758–762.

[2] Bird, R.E.; Hulstrom, R.L. *A Simplified Clear Sky Model for Direct and Diffuse Insolation on Horizontal Surfaces*. SERI/TR-642-761. Golden, CO: Solar Energy Research Institute, 1981.

[3] Gueymard, C. "Clear-sky irradiance predictions for solar resource mapping and large-scale applications: Improved validation methodology and detailed performance analysis of 18 broadband radiative models." *Solar Energy* (86:8), 2012; pp. 2145–2169.

[4] PV_LIB MATLAB Framework. Available online: http://pvpmc.org/pv-lib/.

[5] Blanco-Muriel, M., et al. "Computing the solar vector." *Solar Energy* (70:5), 2001; pp. 431–441. Available online: http://www.psa.es/sdg/sunpos.htm

[6] Gueymard, C. "Analysis of monthly average atmospheric precipitable water and turbidity in Canada and northern United States." *Solar Energy* (53:1), 1994; pp. 57–71.

[7] Gueymard, C. "SMARTS2, simple model of the atmospheric radiative transfer of sunshine: Algorithms and performance assessment." FSEC-PF-270-95. Cocoa, FL: Florida Solar Energy Center, 1995.

This report is available at no cost from the National Renewable Energy Laboratory (NREL) at www.nrel.gov/publications.

Appendix A

Optical Depth Effect on Irradiance

All three clear sky models require a measure of the atmospheric optical depth (AOD) to determine the attenuation or "extinction" of extraterrestrial radiation as it passes through the atmosphere. The exponential law of solar radiation extinction takes the form

$$I(\lambda) = I_0(\lambda)e^{-\frac{\tau(\lambda)}{\cos(\theta)}} \quad (1)$$

where $I_0(\lambda)$ is the extraterrestrial flux at wavelength(λ), $I(\lambda)$ is the flux reaching the ground, θ is the solar zenith angle, and $\tau(\lambda)$ is the optical depth of the vertical column of atmosphere over the observation location at that wavelength. The total optical depth is typically comprised of three components: Raleigh scattering, aerosols, and atmospheric gas absorption, typically shown as

$$\tau(\lambda) = \tau_R(\lambda) + \tau_{AOD}(\lambda) + \tau_g(\lambda) \quad (2)$$

Raleigh optical depth, τ_R, is the scattering of light due to individual molecules in the atmosphere and is a very strong driver of solar radiation extinction. In general, τ_R varies as λ^{-4} and can be relatively easily estimated from atmospheric pressure. Although τ_R is an important extinction term, it doesn't figure into model sensitivities because it is so easily and accurately determined for any site.

Aerosol optical depth, τ_{AOD}, is a measure of the scattering and absorption of light by dust and haze and is the second most important contributor to radiation extinction after Raleigh scattering. Its extinction percentage over the whole spectrum is often the same order of magnitude as Raleigh scattering. It is the most complex atmospheric parameter to accurately estimate and strongly affects clear sky calculations, as aerosol extinction is typically large in the middle of the visible spectrum where the solar irradiance is highest. AOD is generally a smooth extinction function dependent on wavelength

$$\tau(\lambda) = \beta\lambda^{-\alpha} \quad (3)$$

where α and β are called the Angstrom exponent and Angstrom turbidity coefficient, respectively, and can be determined empirically from satellite data (e.g., NASA MODIS data product) or from surface-based narrow-band radiometers, such as the MFRSR or sun photometer found in the NOAA SURFRAD or NASA AERONET (AErosol RObotic NETwork) systems, respectively.

Finally, gaseous optical depth, τ_g, is radiation extinction due to absorption by atmospheric gases (H_2O, ozone, N_2). The most important of these is water column, which has strong absorption bands in the near-infrared. Water column is site dependent and can be estimated using the method by Gueymard [6] using surface measurements of temperature and relative humidity. Alternatively, water column can be estimated from satellite measurements (e.g., NASA MODIS data products). Ozone and nitrogen are two other contributors, but for these clear sky models, fixed values as recommended by the authors have provided sufficient accuracy.

This report is available at no cost from the National Renewable Energy Laboratory (NREL) at www.nrel.gov/publications.

The spectral distribution of the extinction of direct radiation by each of these constituents is shown graphically in the figure below. The data for this figure is taken from the NREL SMARTS model developed by Gueymard [7] using typical atmospheric conditions. Originally detailed in Section 3, the reason for the particular model sensitivities is now more evident. Aerosols drive the radiation extinction, followed by Rayleigh scattering, water column, and ozone absorption. Other atmospheric gases (N_2, O_2, NO_2) also contribute to this attenuation, but to a much lesser degree. Most clear sky models neglect or simply combine the contribution of these less important constituents.

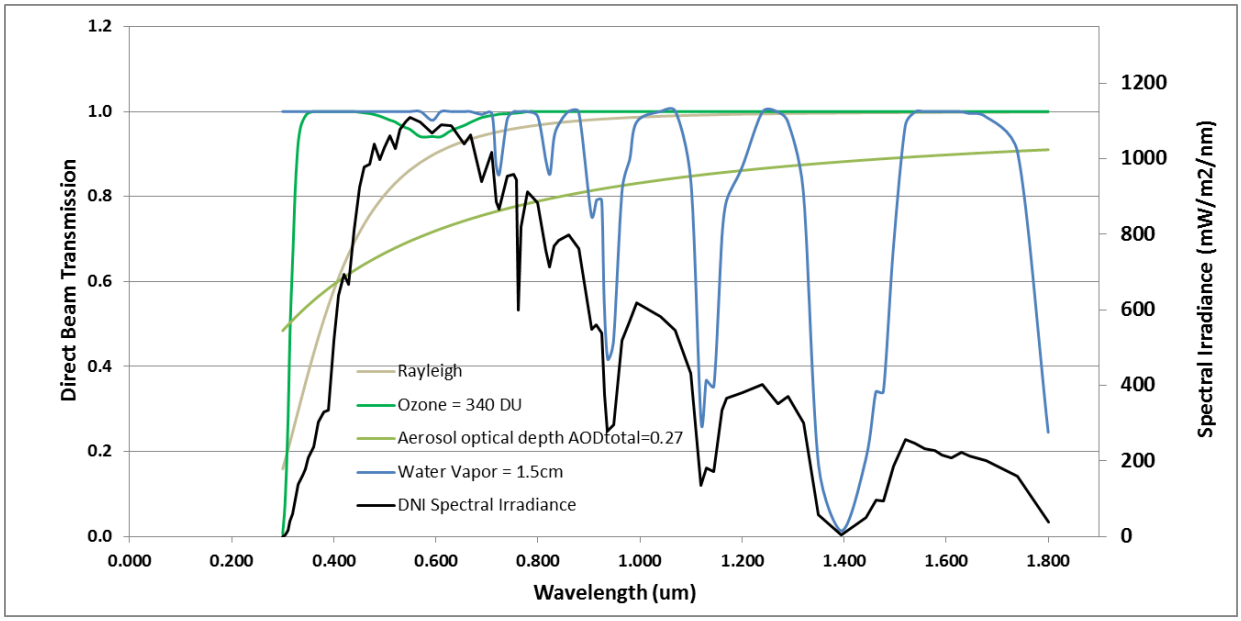

Figure A1. Direct solar transmission of major components of the clear sky atmosphere superimposed on spectral DNI for the same conditions.

Determination of Angstrom Turbidity Coefficients for Model Validation

For this model validation work, the clear sky models require inputs of either τ_{AOD} at specific wavelengths (Bird, SolisBB) or the Angstrom exponent and turbidity coefficient α and β (REST2). Using the relationship in Equation (3), the natural log of each side can be taken, resulting in:

$$\ln(\tau_\lambda) = \ln(\beta) - \alpha \cdot \ln(\lambda) \qquad (4)$$

This equation has the form of a linear equation for λ measured in microns. In a stable atmosphere, this results in a straight line with an intercept of $\beta = \tau$ ($\lambda = 1$ μm) and slope α. Once α and β are determined, the AOD at any specified wavelength can be calculated from Equation (3).

Surface-measured τ_{AOD} is required for clear sky model validation. The narrow-band radiometer that performs this measurement is the SURFRAD MFRSR and its associated data stream. The MFRSR makes simultaneous measurements of the solar irradiances at six wavelengths (nominally 415 nm, 500 nm, 615 nm, 673 nm, 868 nm, and 940 nm) at one-minute intervals

This report is available at no cost from the National Renewable Energy Laboratory (NREL) at www.nrel.gov/publications.

throughout the day. Time series of direct solar beam extinctions and horizontal diffuse fluxes are derived from these measurements, as well as AOD at each of these wavelengths. Only the 500-nm and 868-nm channels are used to calculate the Angstrom turbidity coefficients. The choice of the 500-nm and 868-nm MFRSR channels for computation of α and β is explained by the instrument co-developer Joseph Michalsky of NOAA. He states that "those are the most trusted channels as they have little to no ozone correction, and, more importantly, they do not typically show light leakage that the two 600's have in the past. … Also, 415 is typically noisier because of the response of the silicon detector."

As an example, a single one-minute measurement from the MFRSR at Desert Rock, Nevada, for May 20, 2009, at 9:00 a.m. is shown below on a $\ln(\lambda_i)$ vs. $\ln(AOD_i)$ scale for the following data:

T.able A1. Desert Rock τ_{AOD} Values from the MFRSR

Wavelength [µm]	Measured AOD
0.415	0.1
0.501	0.089
0.616	0.061
0.672	0.059
0.868	0.051

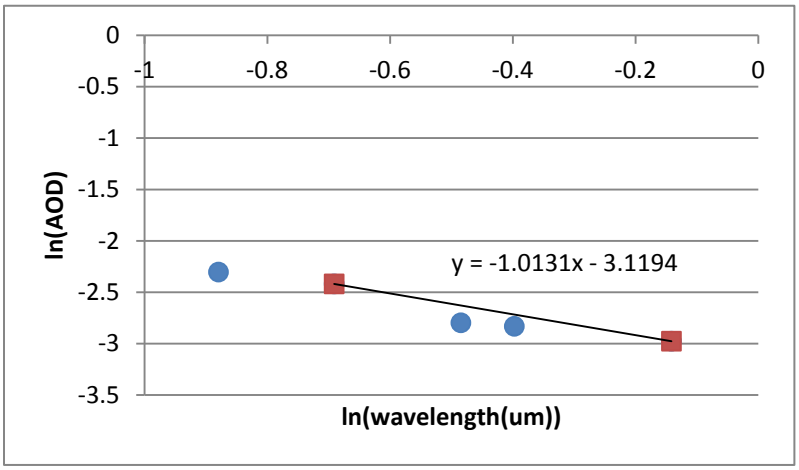

Figure A2. Determination of Angstrom turbidity coefficients.

Calculating the line between AOD at 500 nm and 868 nm gives a slope of -1.013 and y-intercept at -3.12. Angstrom exponent α is defined as the negative of the slope. Hence, α = 0.986. The y-intercept is lnβ = -3.12. Hence, the Angstrom turbidity coefficient $\beta = e^{-3.12} = 0.044$. Gueymard makes the further distinction that α and β be determined separately above and below 7 µm for REST2. However, for this analysis it was assumed the slope and intercept were the same for AOD above and below 7 µm, which Gueymard recommends when additional spectral data is not available.

A final screening measure recommended by Gueymard was used to limit potentially bad measured data. Here, α was limited to within 0.3 and 2.5 and β limited to within 0.001 and 0.5. Any α, β pairs outside this range were replaced with annual climatic values.

This report is available at no cost from the National Renewable Energy Laboratory (NREL) at www.nrel.gov/publications.

The SURFRAD AOD data was processed to create both a daily and an annual climatic dataset for all the SURFRAD stations. The daily value dataset is the daily average of the one-minute AODs for the entire 2009 analysis year, excluding any data flagged as bad, which includes any cloudy periods. Any missing days are replaced with the annual average. The annual dataset consists of the annual mean climatic values for all flagged good measurements in 2009. These datasets were the basis of the AOD data used for the clear sky model evaluations.

This report is available at no cost from the National Renewable Energy Laboratory (NREL) at www.nrel.gov/publications.

Appendix B

Data Flow for Clear Sky Model Evaluation

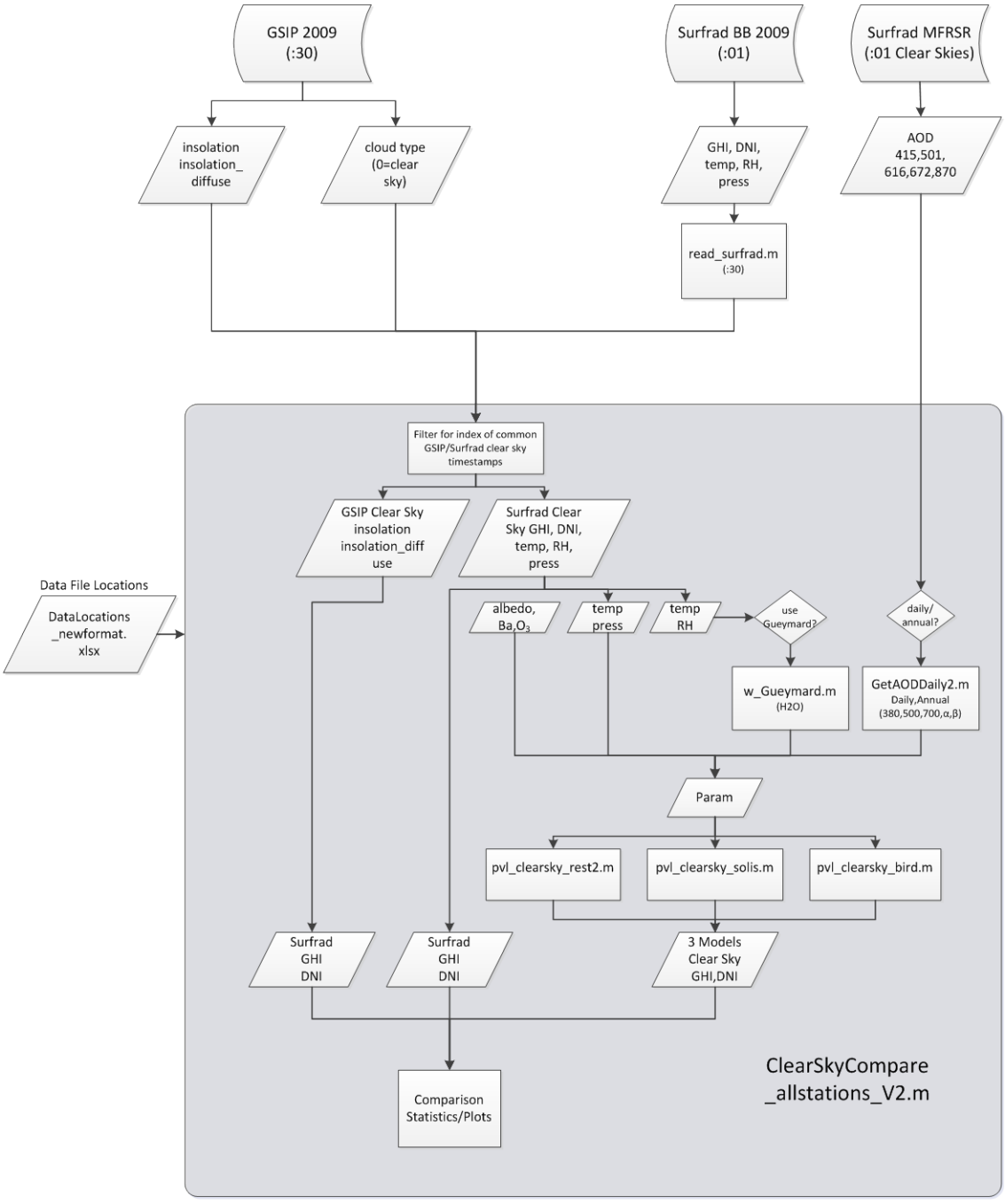

This report is available at no cost from the National Renewable Energy Laboratory (NREL) at www.nrel.gov/publications.

Appendix C

Model Improvement Due to Use of Daily AOD and Half-Hour Water Column

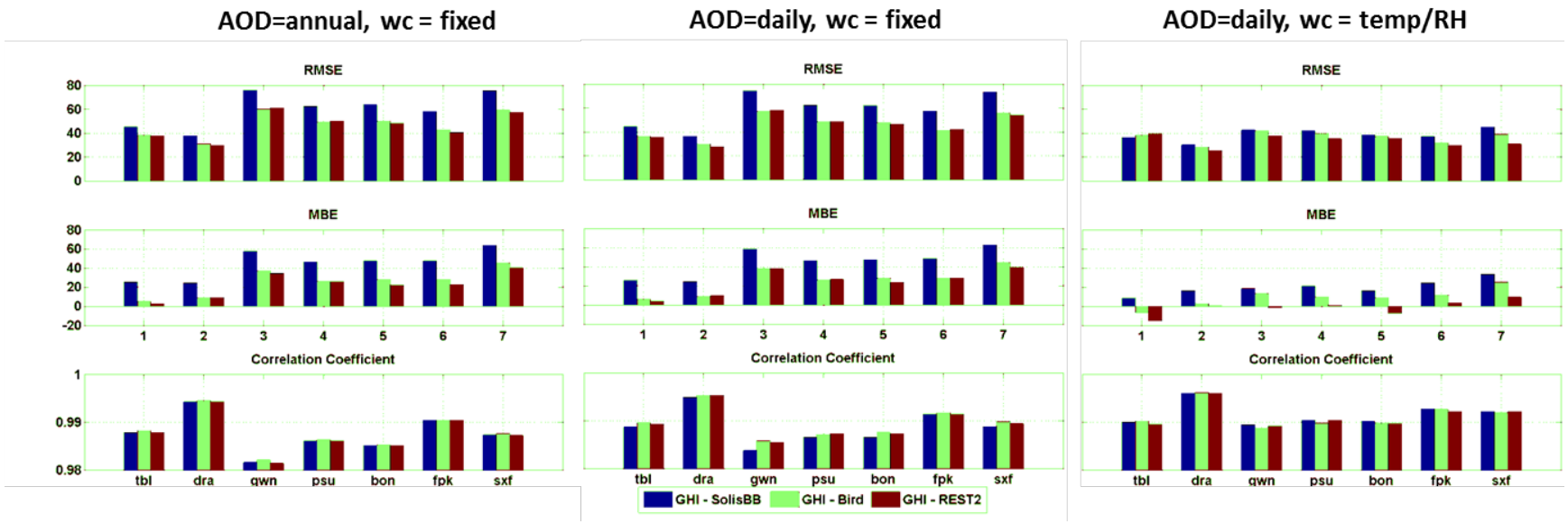

GHI

This report is available at no cost from the National Renewable Energy Laboratory (NREL) at www.nrel.gov/publications.

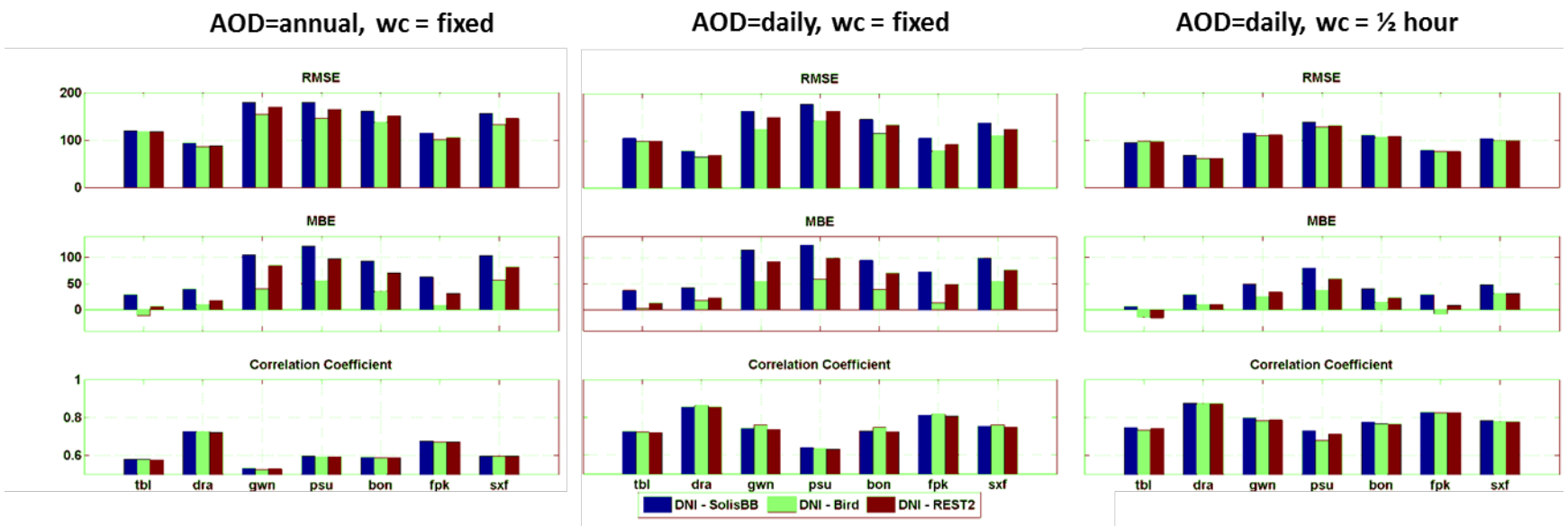

DNI

This report is available at no cost from the National Renewable Energy Laboratory (NREL) at www.nrel.gov/publications.

Appendix D

GHI Clear Sky Model Comparisons for All Sites

Table Mountain GHI

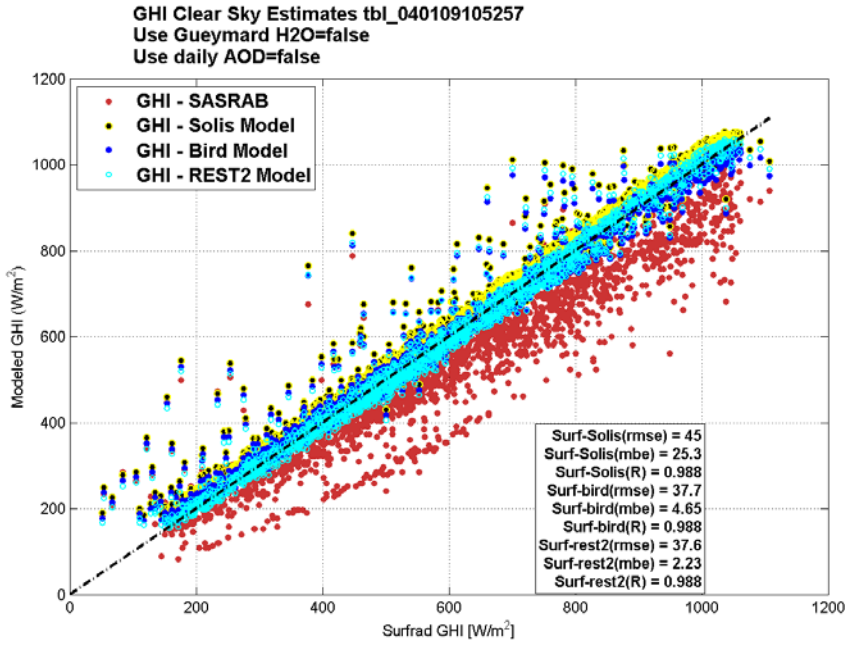

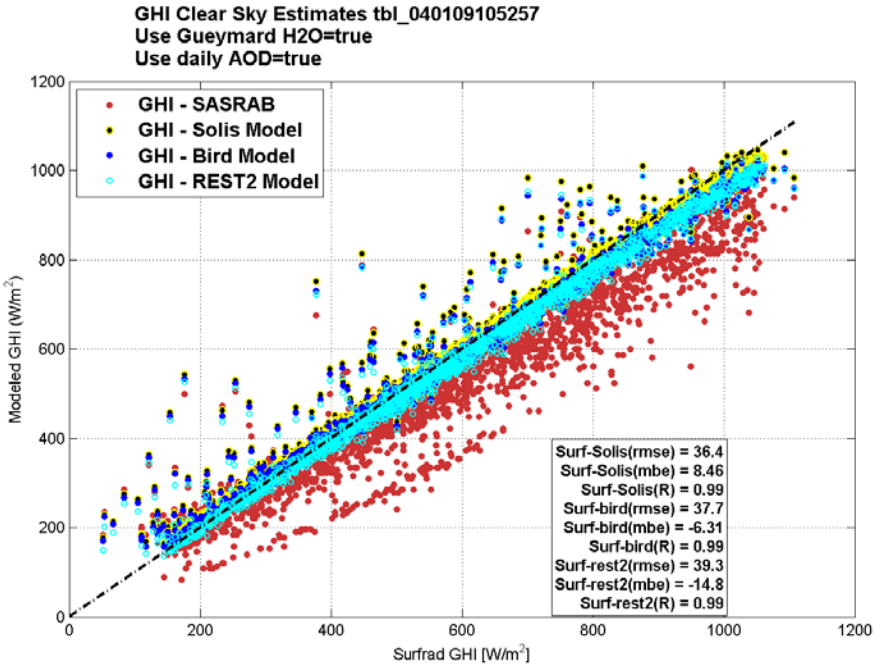

This report is available at no cost from the National Renewable Energy Laboratory (NREL) at www.nrel.gov/publications.

Table Mountain DNI

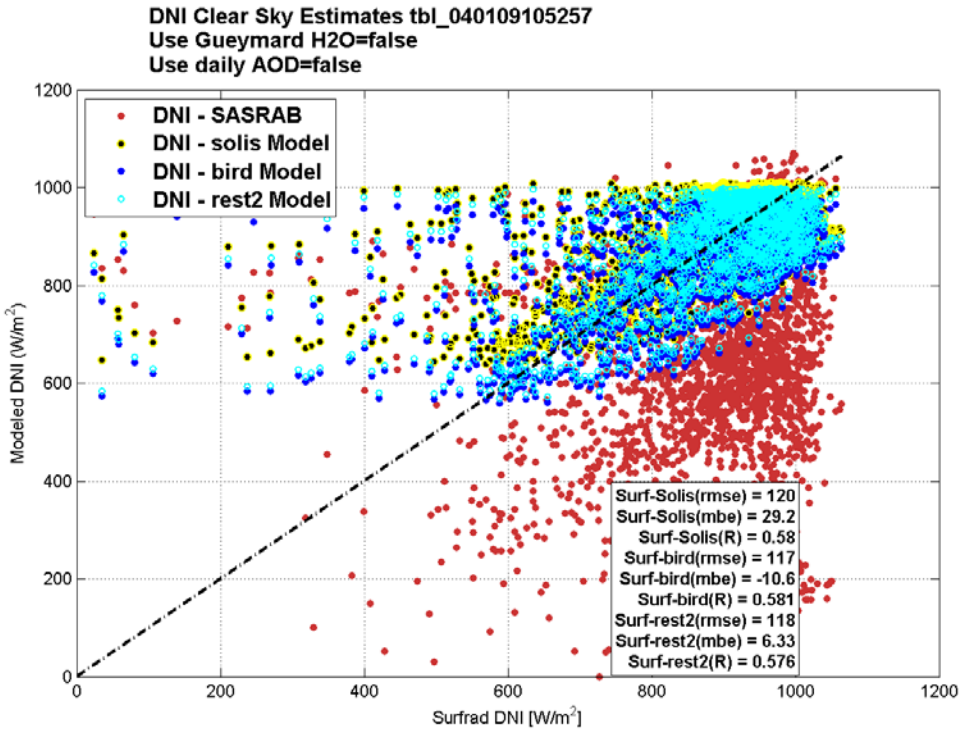

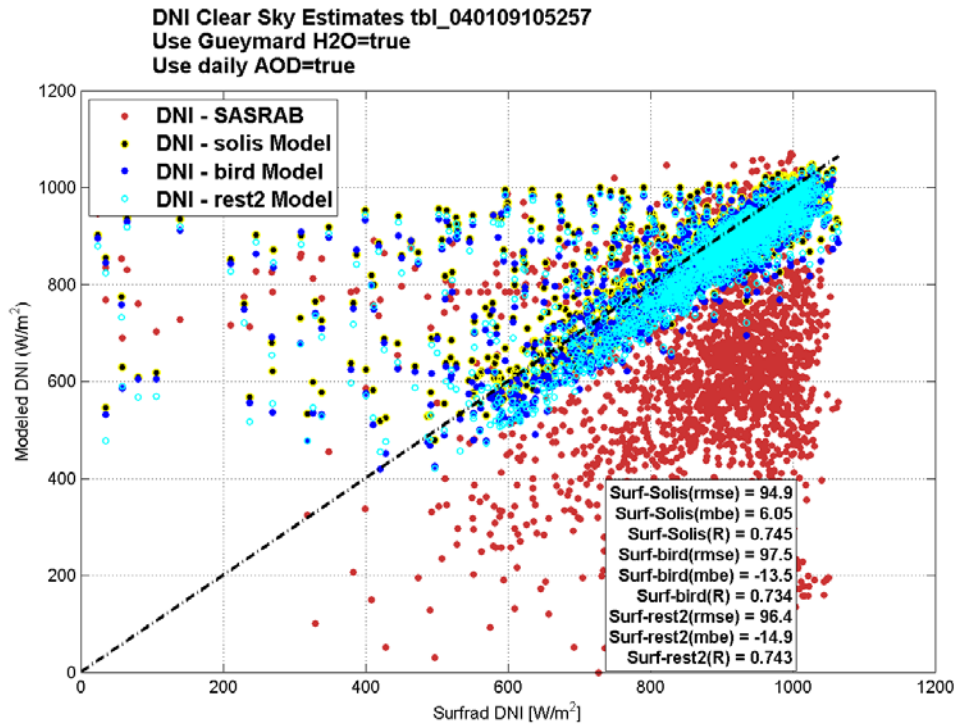

This report is available at no cost from the National Renewable Energy Laboratory (NREL) at www.nrel.gov/publications.

Desert Rock GHI

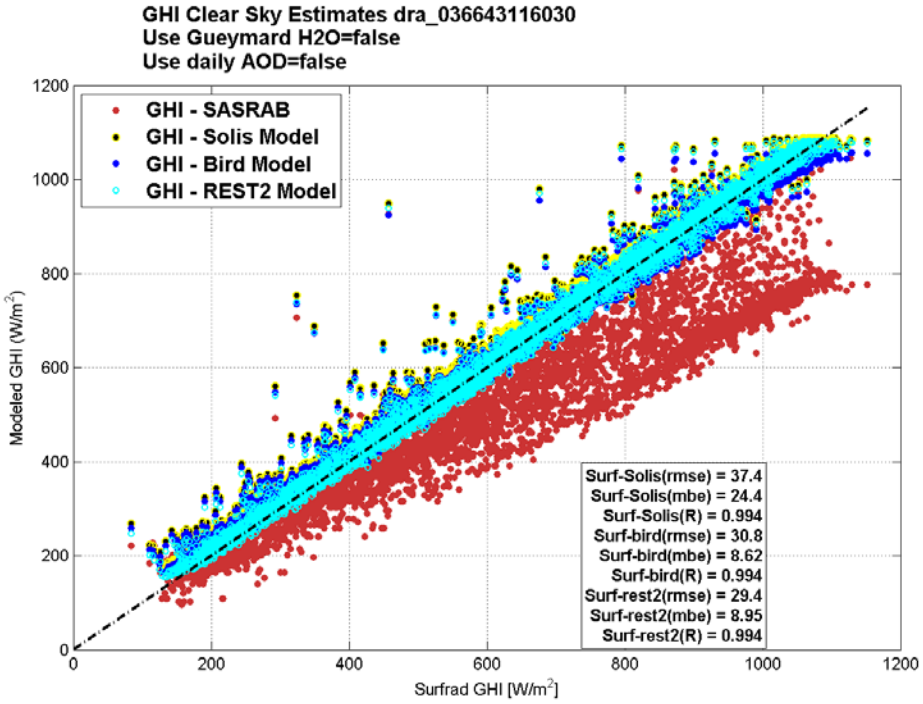

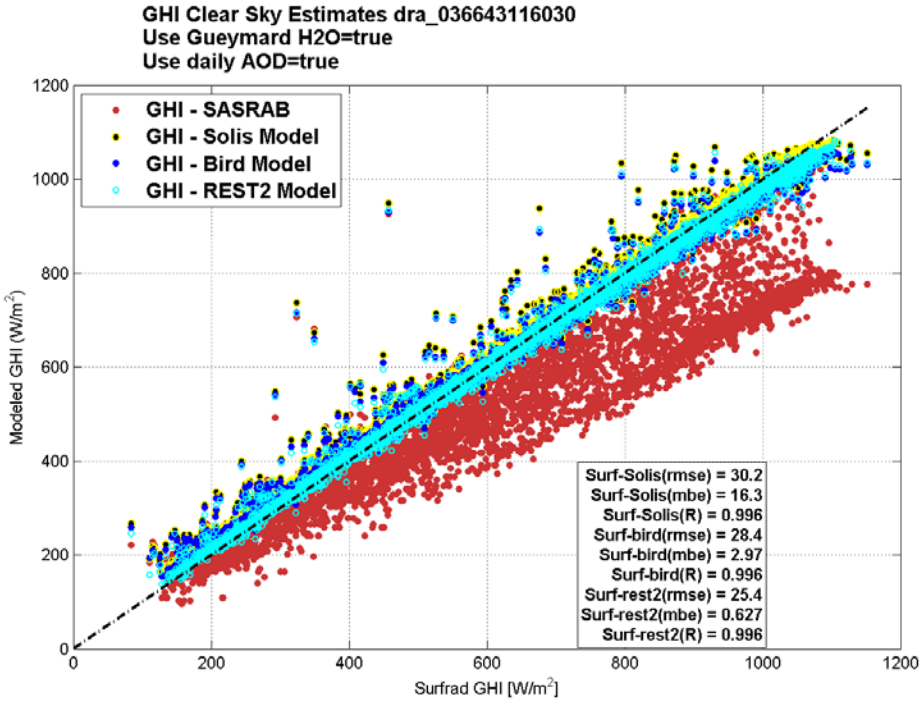

This report is available at no cost from the National Renewable Energy Laboratory (NREL) at www.nrel.gov/publications.

Desert Rock DNI

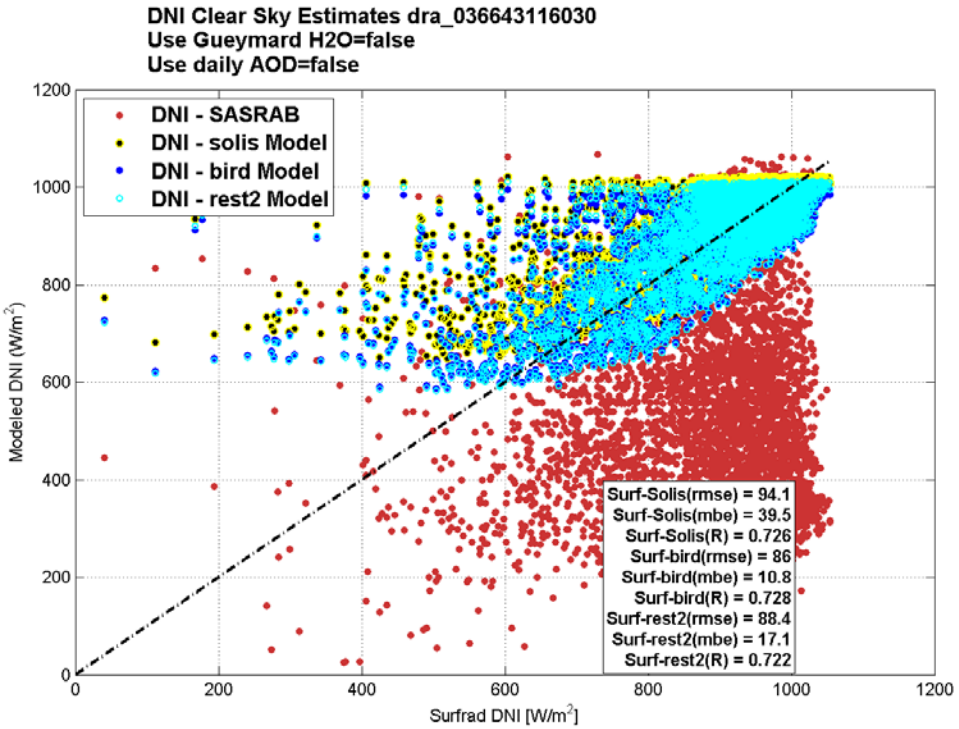

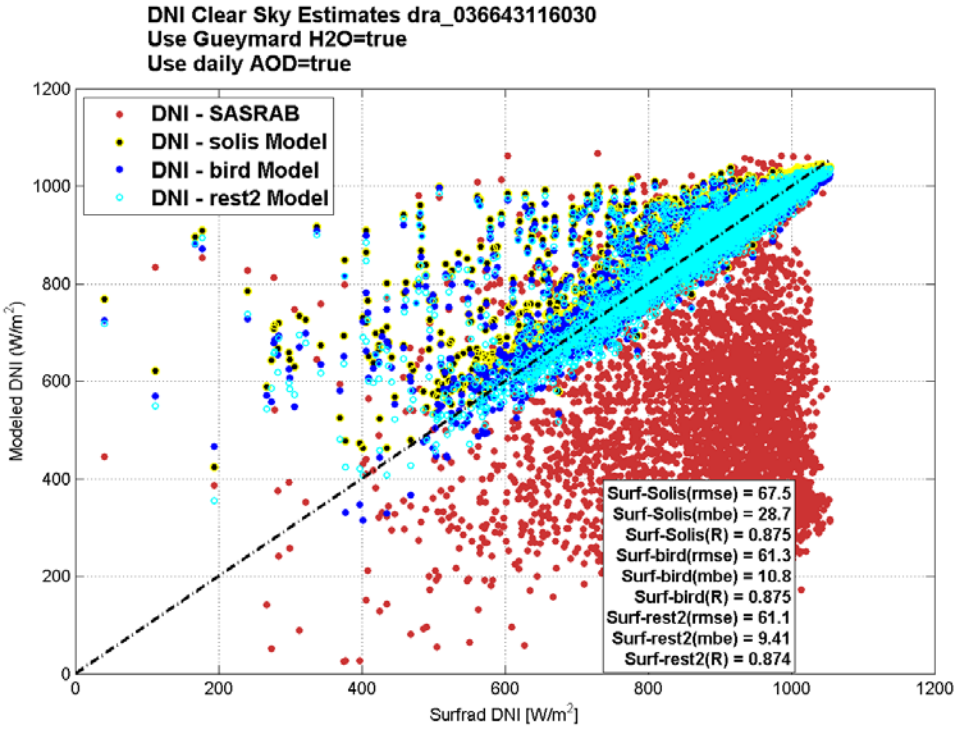

This report is available at no cost from the National Renewable Energy Laboratory (NREL) at www.nrel.gov/publications.

Goodwin Creek GHI

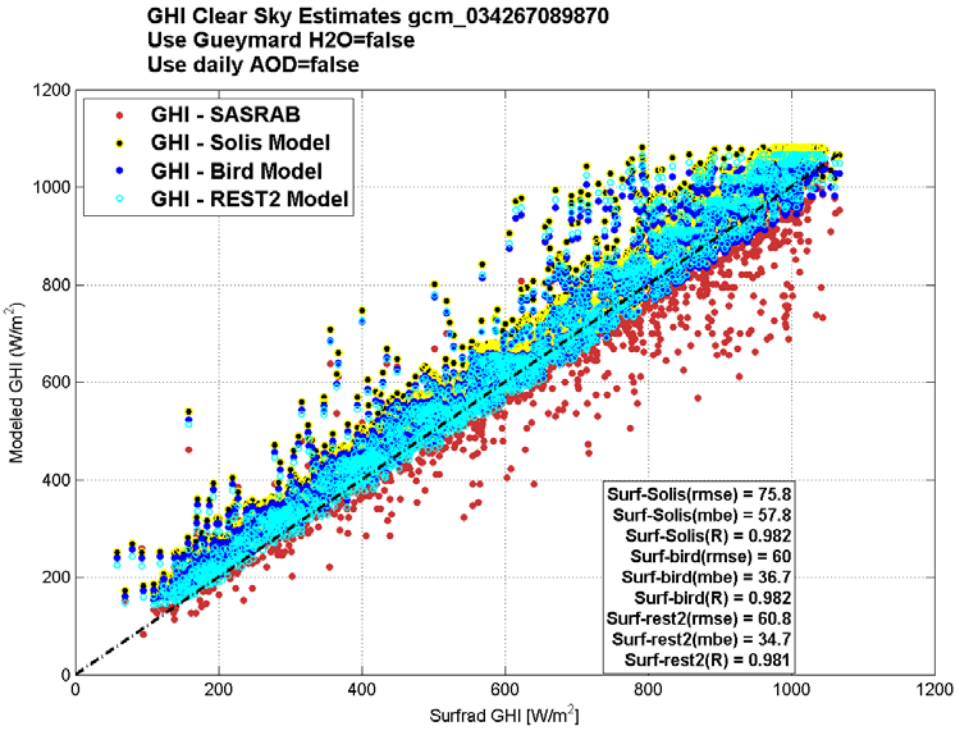

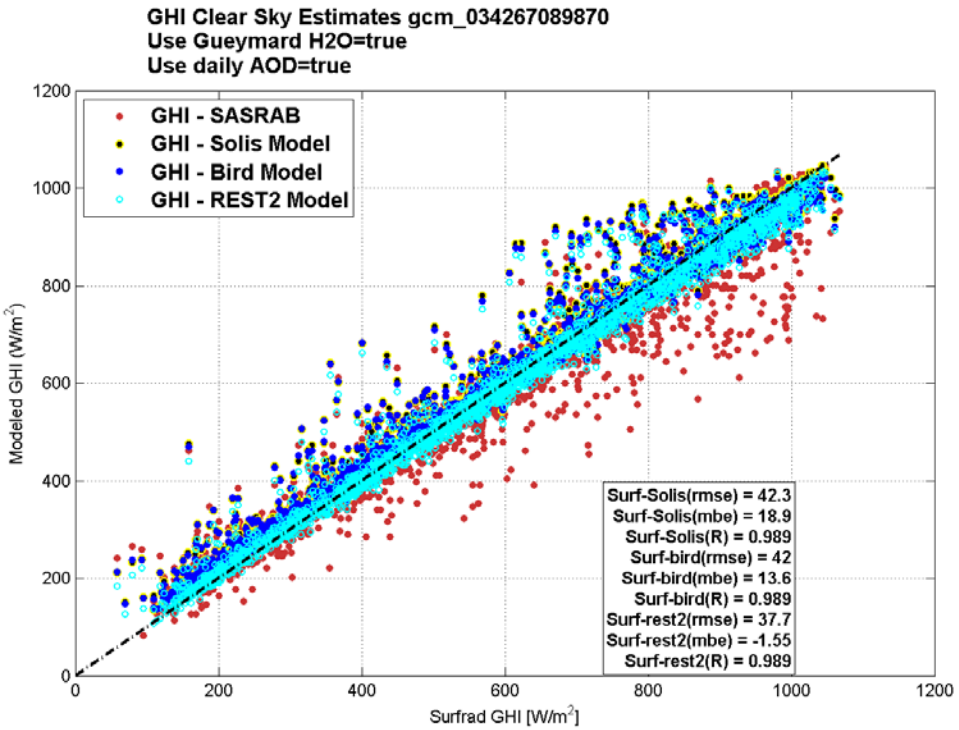

This report is available at no cost from the National Renewable Energy Laboratory (NREL) at www.nrel.gov/publications.

Goodwin Creek DNI

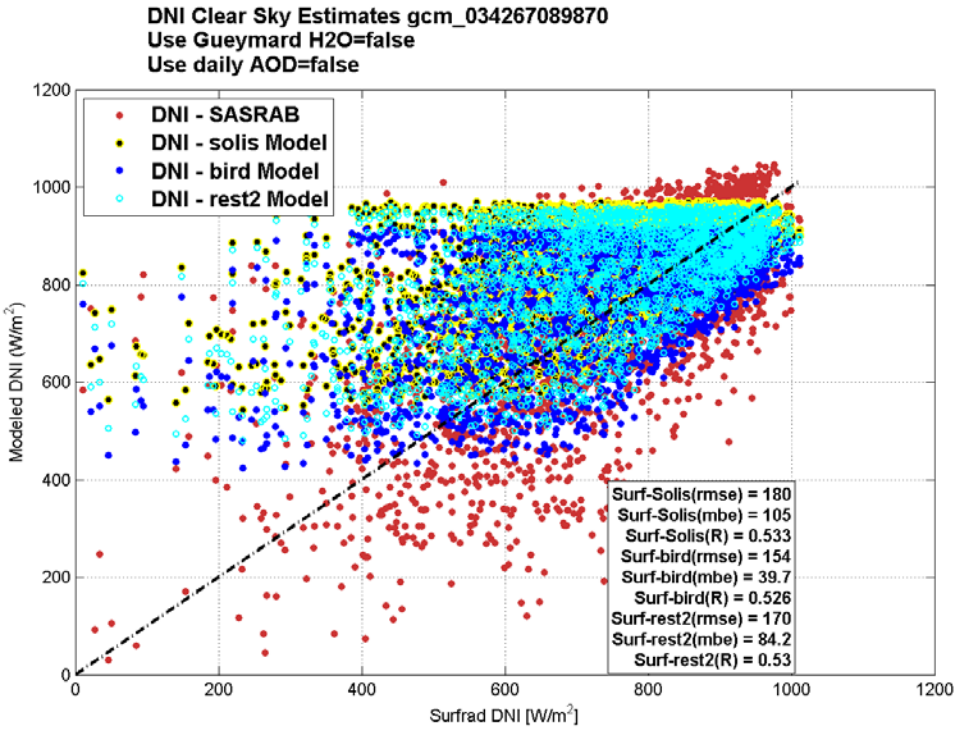

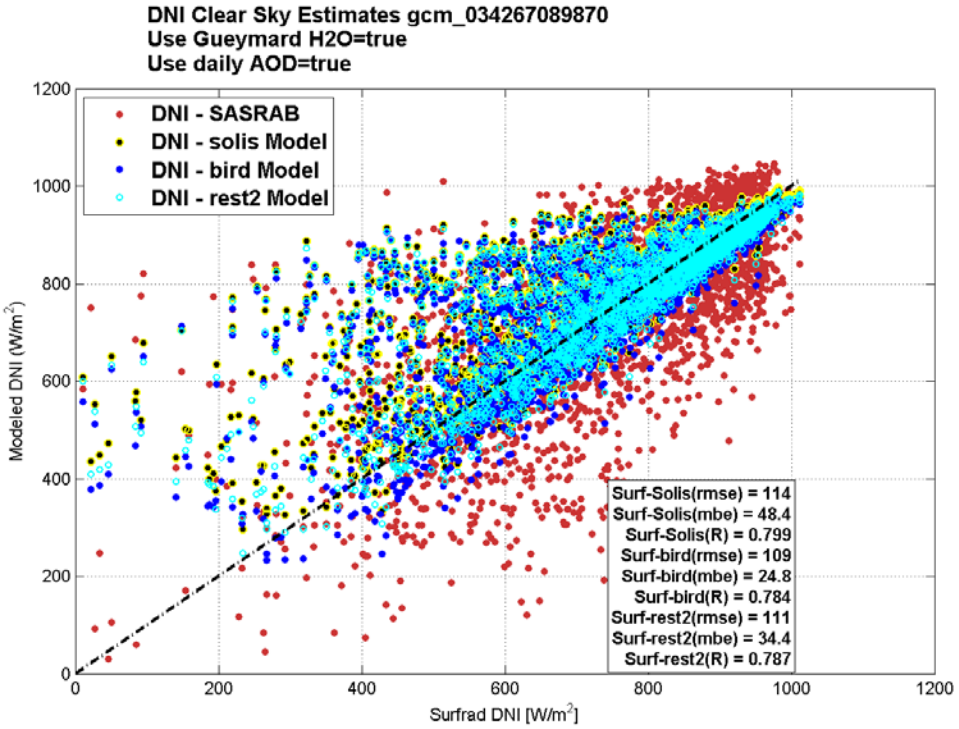

This report is available at no cost from the National Renewable Energy Laboratory (NREL) at www.nrel.gov/publications.

Penn State GHI

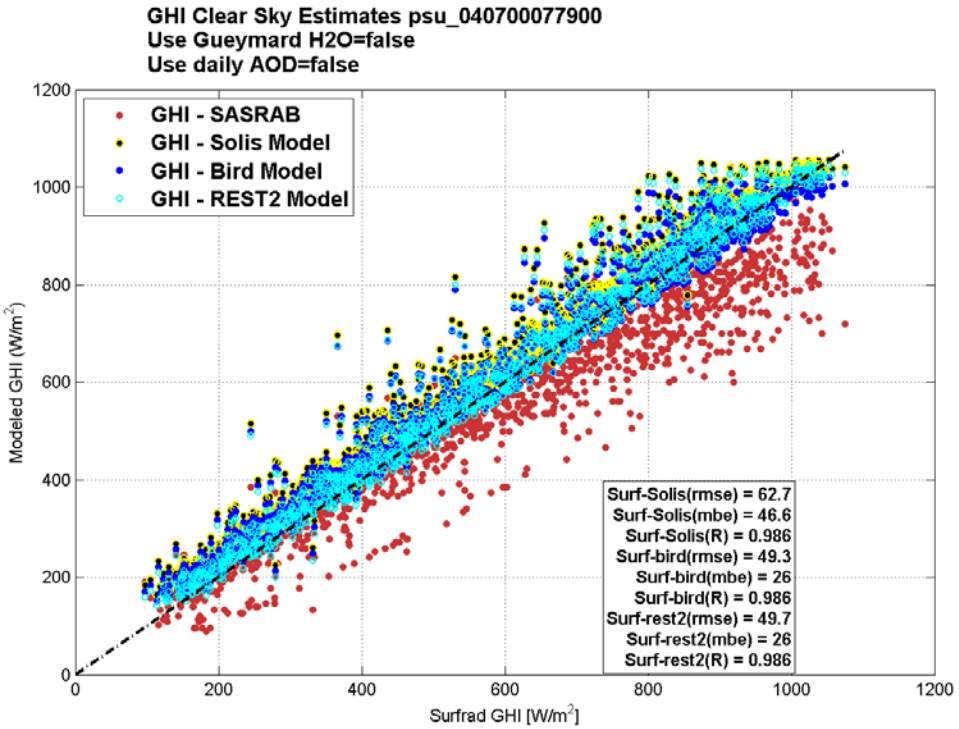

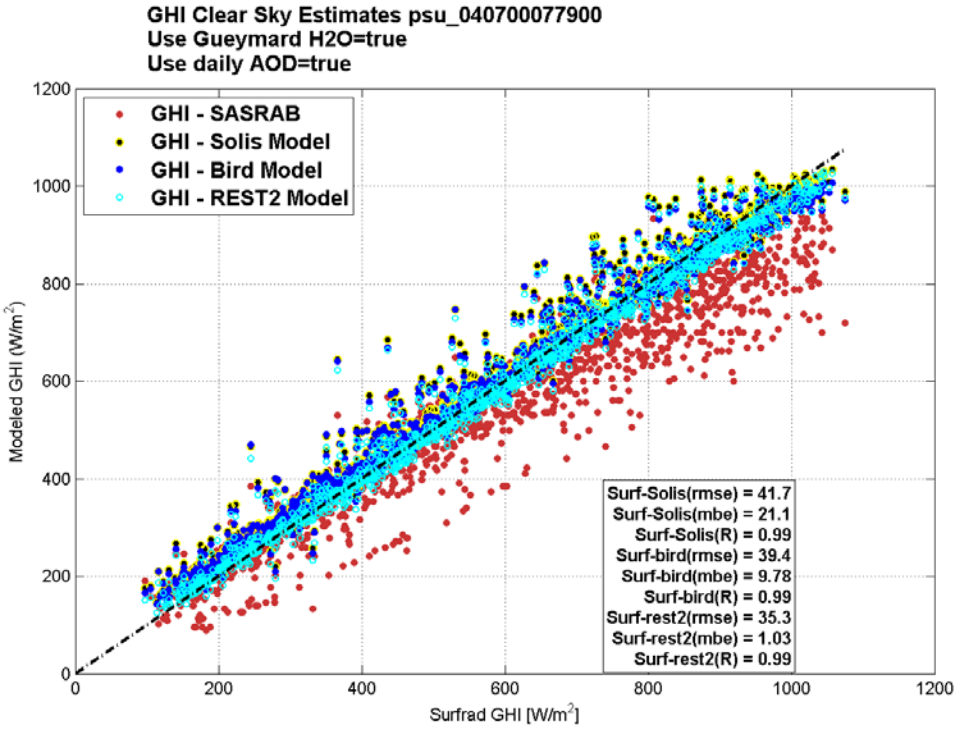

This report is available at no cost from the National Renewable Energy Laboratory (NREL) at www.nrel.gov/publications.

Penn State DNI

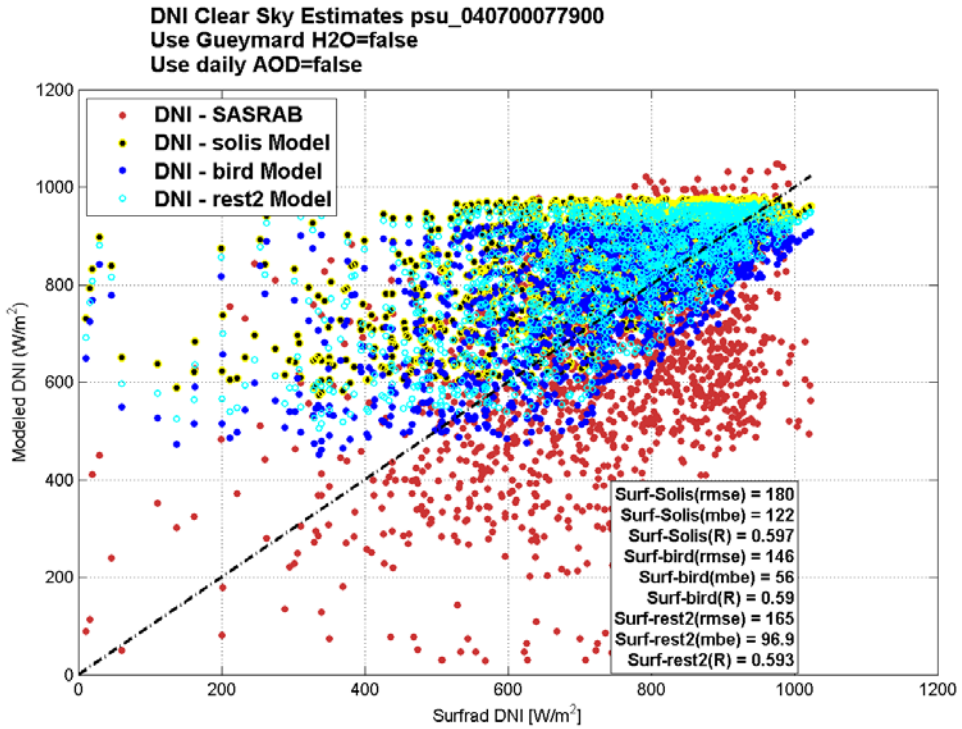

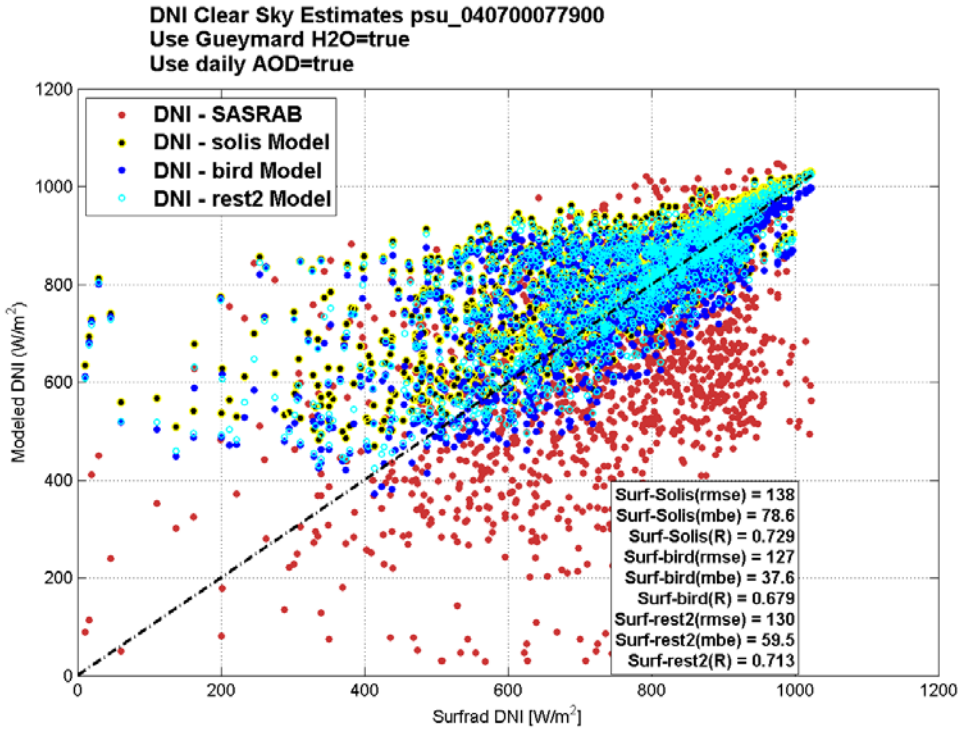

This report is available at no cost from the National Renewable Energy Laboratory (NREL) at www.nrel.gov/publications.

Bondville GHI

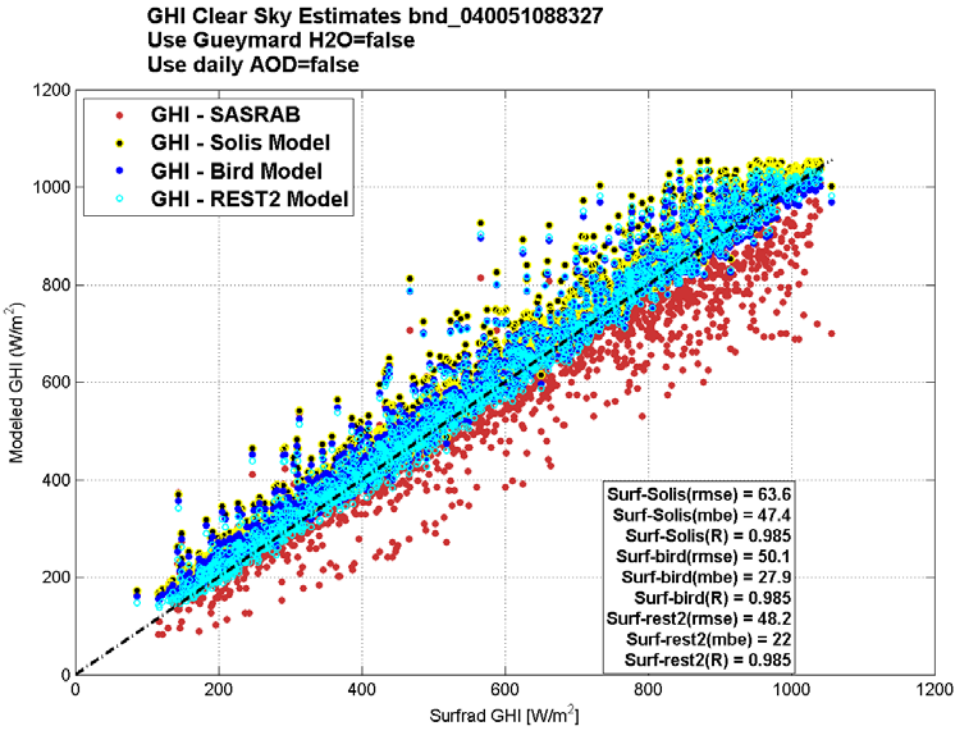

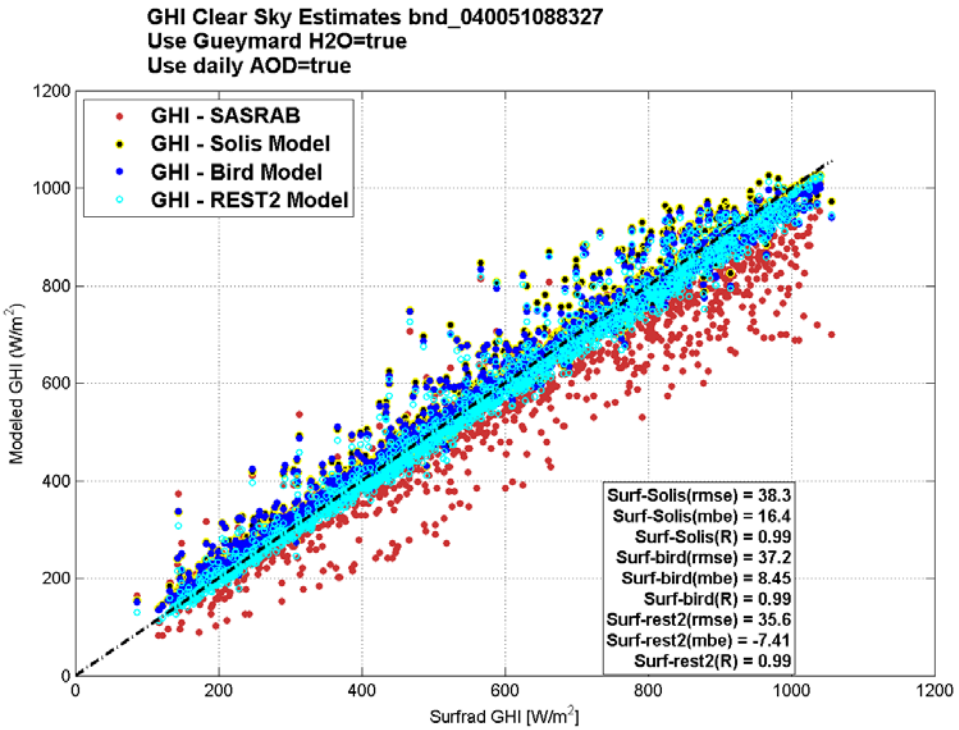

This report is available at no cost from the National Renewable Energy Laboratory (NREL) at www.nrel.gov/publications.

Bondville DNI

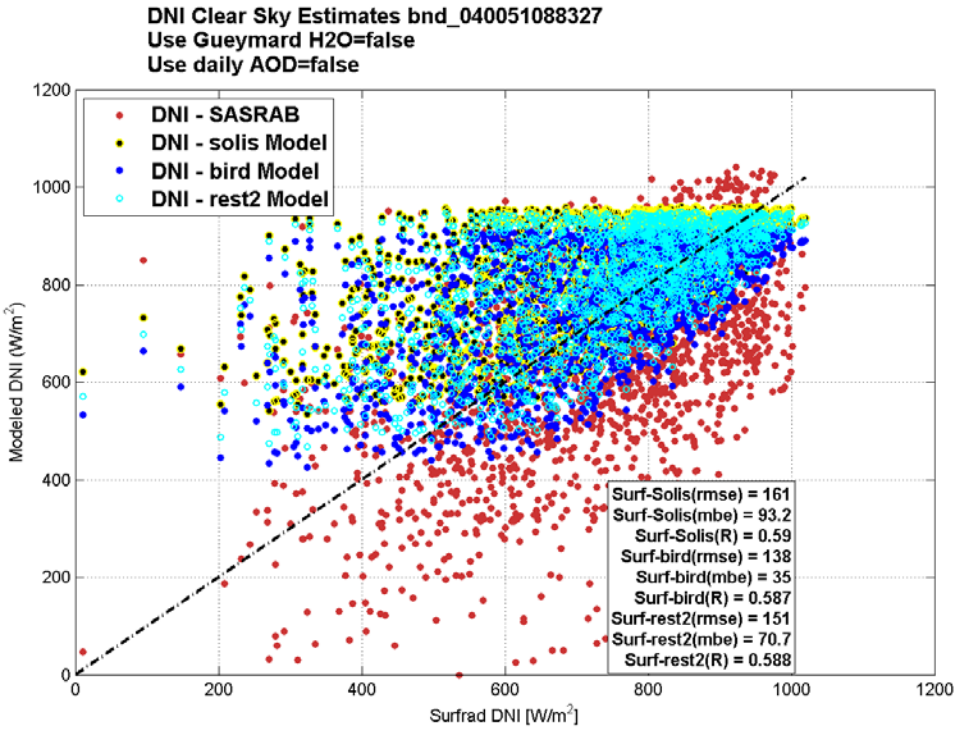

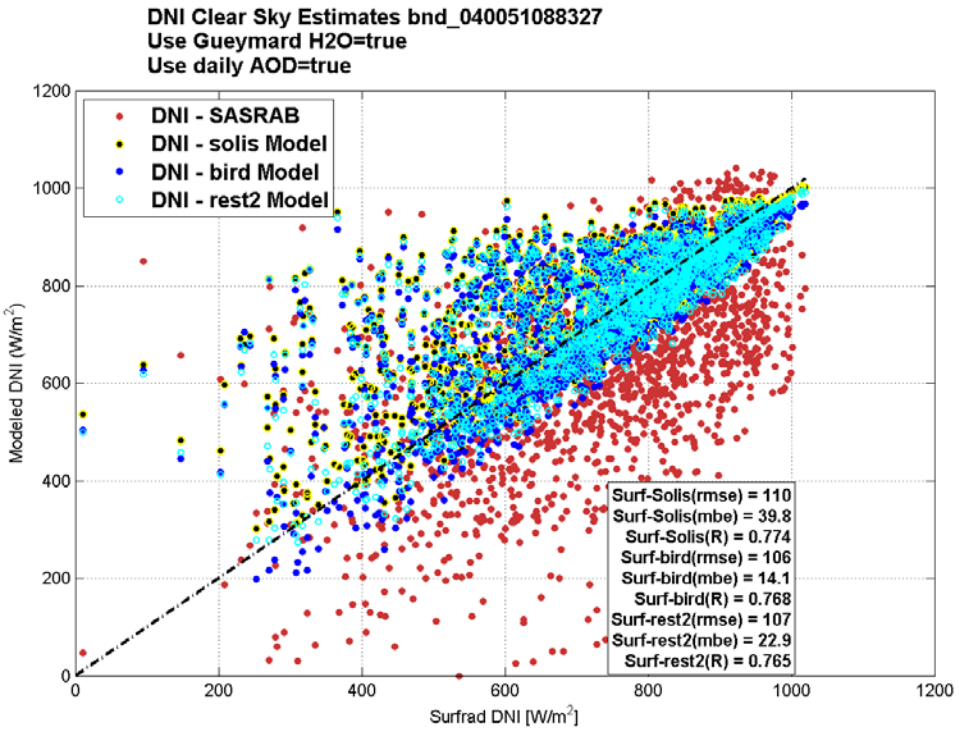

This report is available at no cost from the National Renewable Energy Laboratory (NREL) at www.nrel.gov/publications.

Fort Peck GHI

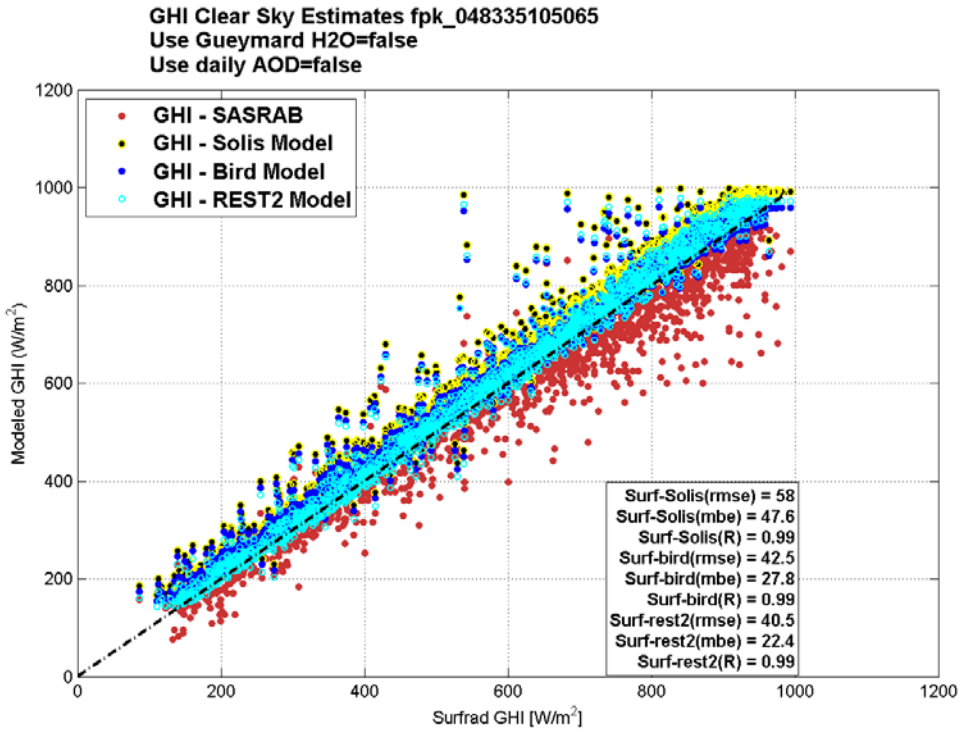

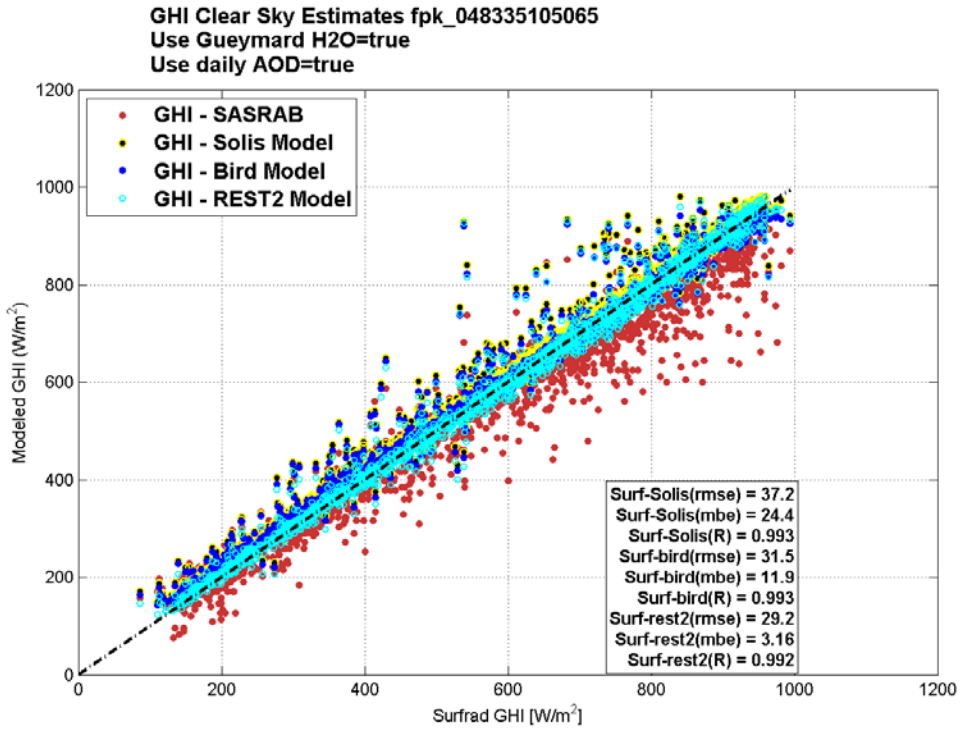

This report is available at no cost from the National Renewable Energy Laboratory (NREL) at www.nrel.gov/publications.

Fort Peck DNI

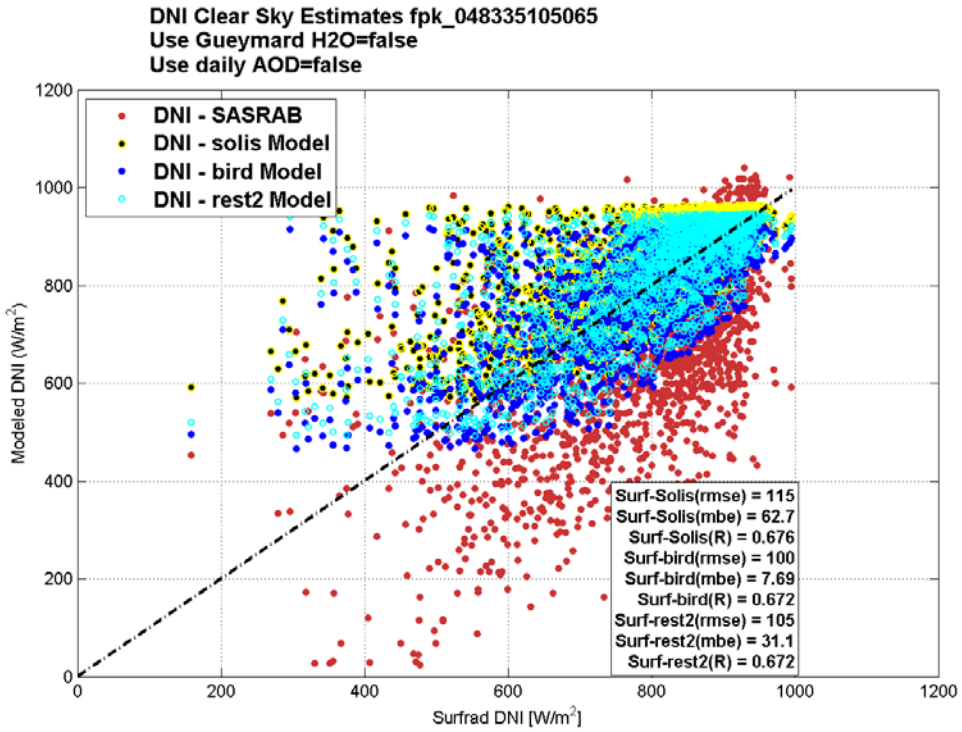

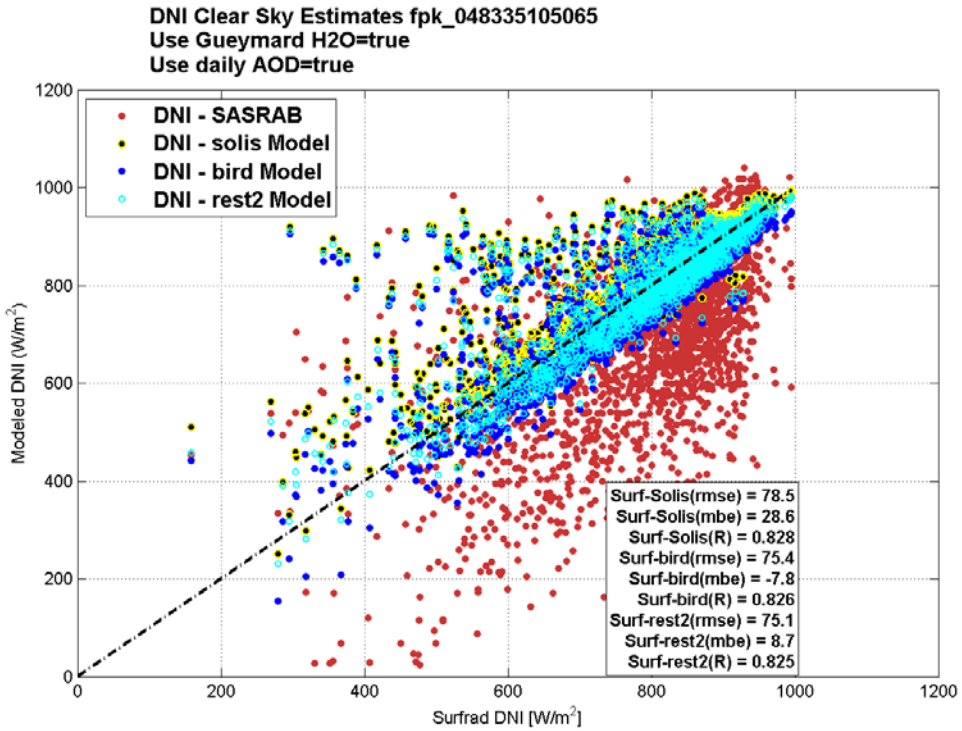

This report is available at no cost from the National Renewable Energy Laboratory (NREL) at www.nrel.gov/publications.

Sioux Falls GHI

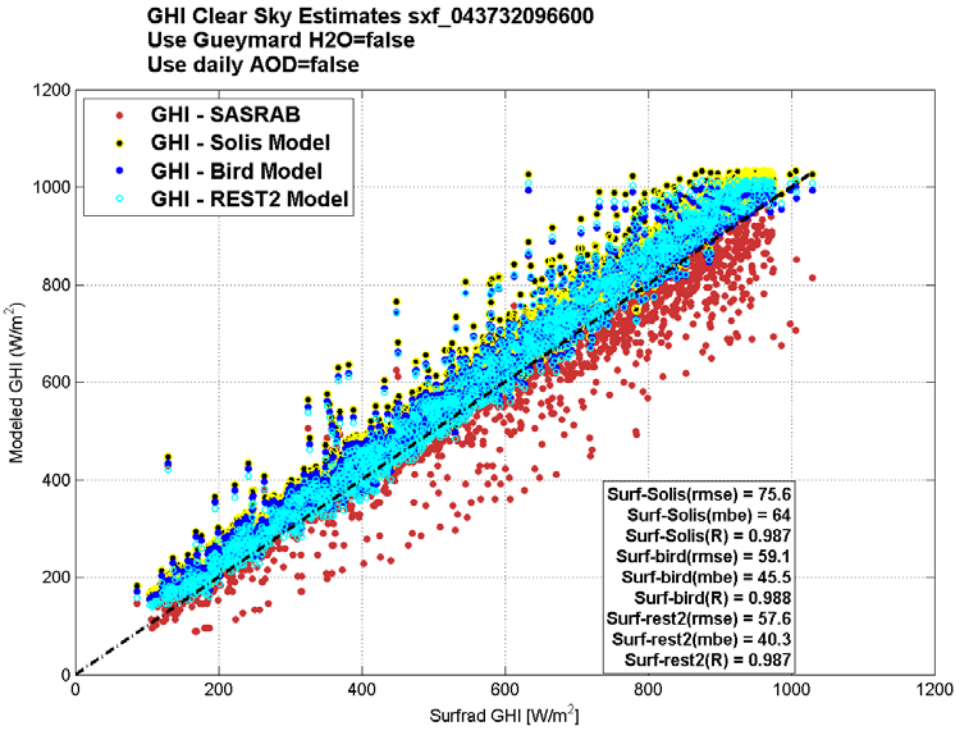

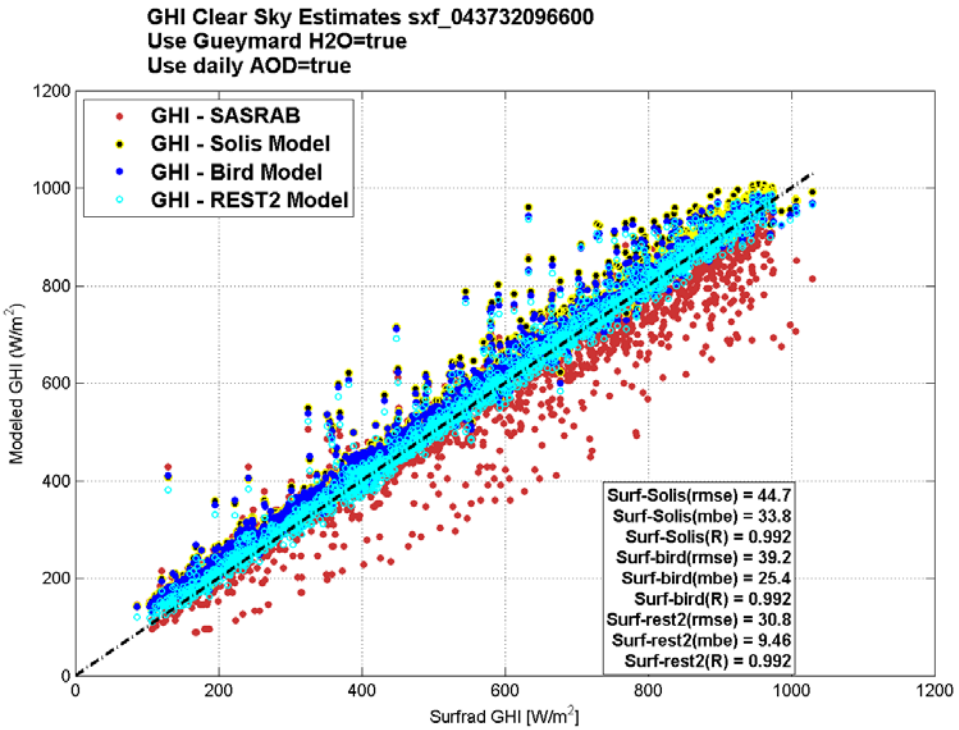

This report is available at no cost from the National Renewable Energy Laboratory (NREL) at www.nrel.gov/publications.

Sioux Falls DNI

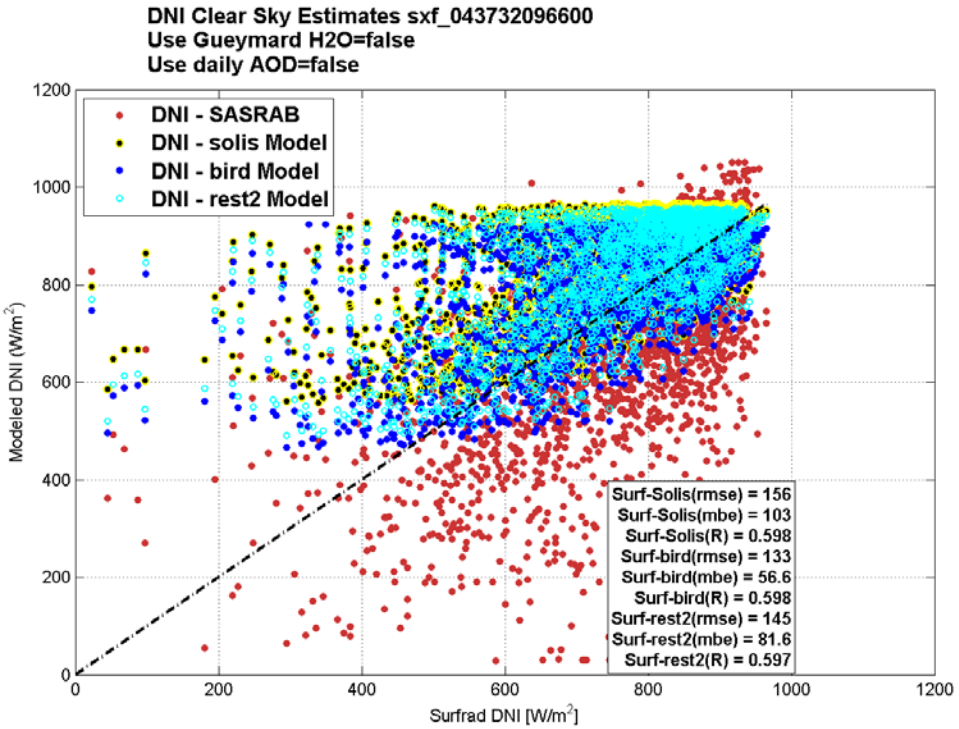

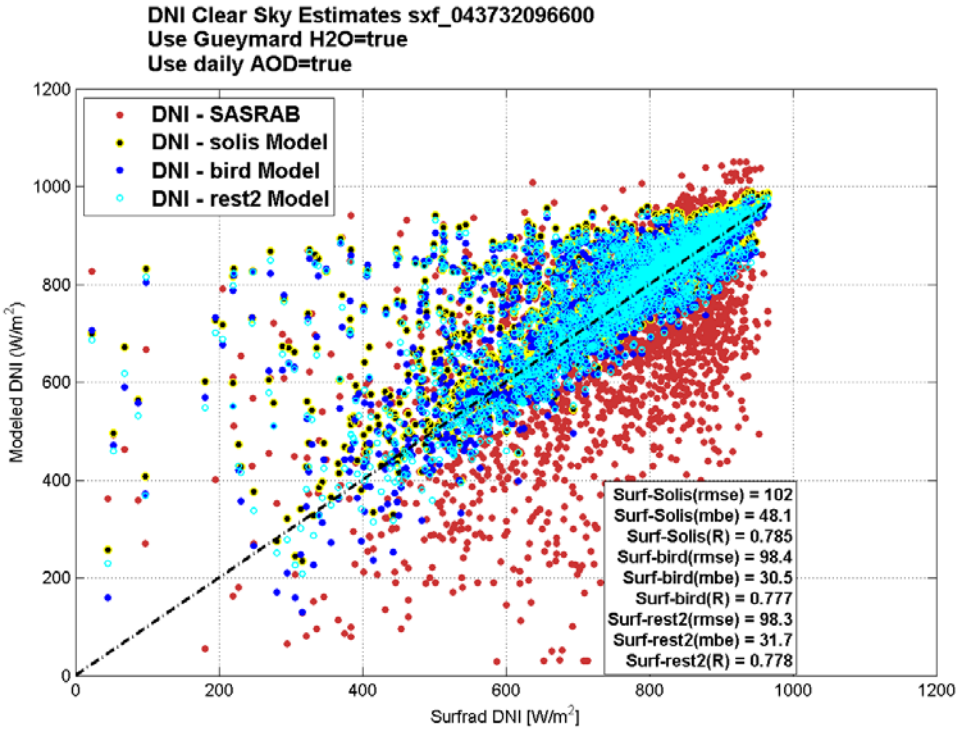

This report is available at no cost from the National Renewable Energy Laboratory (NREL) at www.nrel.gov/publications.